AFRL-AFOSR-VA-TR-2016-0121

Ultrabroadband Phased-array Receivers Based on Optical Techniques

Christopher Schuetz
UNIVERSITY OF DELAWARE

02/26/2016
Final Report

Air Force Research Laboratory
AF Office Of Scientific Research (AFOSR)/ RTA1
Arlington, Virginia 22203
Air Force Materiel Command

REPORT DOCUMENTATION PAGE

Form Approved
OMB No. 0704-0188

PLEASE DO NOT RETURN YOUR FORM TO THE ABOVE ORGANIZATION.

1. REPORT DATE *(DD-MM-YYYY)*	2. REPORT TYPE	3. DATES COVERED *(From - To)*
15-02-2016	Final Performance Report	15 Jul 12 TO 14 Jul 15

4. TITLE AND SUBTITLE
Ultrabroadband Phased-Array Receivers Based on Optical Techniques

5a. CONTRACT NUMBER

5b. GRANT NUMBER
FA9550-12-1-0380

5c. PROGRAM ELEMENT NUMBER

6. AUTHOR(S)
Dr. Christopher A. Schuetz and Brock Overmiller

5d. PROJECT NUMBER

5e. TASK NUMBER

5f. WORK UNIT NUMBER

7. PERFORMING ORGANIZATION NAME(S) AND ADDRESS(ES)
University of Delaware
210 Hullihen Hall
Newark, DE 19716

8. PERFORMING ORGANIZATION REPORT NUMBER
ELEG332291-20151014

9. SPONSORING/MONITORING AGENCY NAME(S) AND ADDRESS(ES)
Air Force Office of Scientific Research
875 N. Randolph Street, Room 3112
Arlington, VA 22203

10. SPONSOR/MONITOR'S ACRONYM(S)

11. SPONSOR/MONITOR'S REPORT NUMBER(S)

12. DISTRIBUTION/AVAILABILITY STATEMENT
Approved for public release: distribution unlimited.

13. SUPPLEMENTARY NOTES

14. ABSTRACT

Military operations require the ability to locate and identify electronic emissions in the battlefield environment. However, developments in RADAR and communications technology are making it harder to effectively identify these broadband and increasingly dynamic emissions. To this end, under this effort a broadband imaging receiver for the location and identification of microwave and millimeter-wave emitters has been developed. This approach utilizes photonic techniques to realize an imaging receiver that enables us to capture and convert signals across an array using photonic modulators, routing these signals to a central location using fiber optics, and spatially and spectrally processing the incoming signals using simple free space optics. Over the course of this effort, the capability of using such an optically enabled imaging receiver array to simultaneously detect, locate, and downconvert multiple high-gain beams in a non-blocking fashion using an optically enabled imaging receiver array has been demonstrated for the first time. This technology was demonstrated first by adapting an existing 35 GHz passive millimeter wave imager that predated this effort, and subsequently by building a four element broadband array, which is capable of detection over the range of 4-50 GHz.

15. SUBJECT TERMS
RF photonics, imaging receiver, electronic warfare, spatial signal processing, millimeter-wave

16. SECURITY CLASSIFICATION OF:			17. LIMITATION OF ABSTRACT	18. NUMBER OF PAGES	19a. NAME OF RESPONSIBLE PERSON
a. REPORT	b. ABSTRACT	c. THIS PAGE			Christopher A. Schuetz
U	U	U	UU	31	19b. TELEPHONE NUMBER *(Include area code)* 610-662-1075

Reset

INSTRUCTIONS FOR COMPLETING SF 298

1. REPORT DATE. Full publication date, including day, month, if available. Must cite at least the year and be Year 2000 compliant, e.g. 30-06-1998; xx-06-1998; xx-xx-1998.

2. REPORT TYPE. State the type of report, such as final, technical, interim, memorandum, master's thesis, progress, quarterly, research, special, group study, etc.

3. DATES COVERED. Indicate the time during which the work was performed and the report was written, e.g., Jun 1997 - Jun 1998; 1-10 Jun 1996; May - Nov 1998; Nov 1998.

4. TITLE. Enter title and subtitle with volume number and part number, if applicable. On classified documents, enter the title classification in parentheses.

5a. CONTRACT NUMBER. Enter all contract numbers as they appear in the report, e.g. F33615-86-C-5169.

5b. GRANT NUMBER. Enter all grant numbers as they appear in the report, e.g. AFOSR-82-1234.

5c. PROGRAM ELEMENT NUMBER. Enter all program element numbers as they appear in the report, e.g. 61101A.

5d. PROJECT NUMBER. Enter all project numbers as they appear in the report, e.g. 1F665702D1257; ILIR.

5e. TASK NUMBER. Enter all task numbers as they appear in the report, e.g. 05; RF0330201; T4112.

5f. WORK UNIT NUMBER. Enter all work unit numbers as they appear in the report, e.g. 001; AFAPL30480105.

6. AUTHOR(S). Enter name(s) of person(s) responsible for writing the report, performing the research, or credited with the content of the report. The form of entry is the last name, first name, middle initial, and additional qualifiers separated by commas, e.g. Smith, Richard, J, Jr.

7. PERFORMING ORGANIZATION NAME(S) AND ADDRESS(ES). Self-explanatory.

8. PERFORMING ORGANIZATION REPORT NUMBER. Enter all unique alphanumeric report numbers assigned by the performing organization, e.g. BRL-1234; AFWL-TR-85-4017-Vol-21-PT-2.

9. SPONSORING/MONITORING AGENCY NAME(S) AND ADDRESS(ES). Enter the name and address of the organization(s) financially responsible for and monitoring the work.

10. SPONSOR/MONITOR'S ACRONYM(S). Enter, if available, e.g. BRL, ARDEC, NADC.

11. SPONSOR/MONITOR'S REPORT NUMBER(S). Enter report number as assigned by the sponsoring/ monitoring agency, if available, e.g. BRL-TR-829; -215.

12. DISTRIBUTION/AVAILABILITY STATEMENT. Use agency-mandated availability statements to indicate the public availability or distribution limitations of the report. If additional limitations/ restrictions or special markings are indicated, follow agency authorization procedures, e.g. RD/FRD, PROPIN, ITAR, etc. Include copyright information.

13. SUPPLEMENTARY NOTES. Enter information not included elsewhere such as: prepared in cooperation with; translation of; report supersedes; old edition number, etc.

14. ABSTRACT. A brief (approximately 200 words) factual summary of the most significant information.

15. SUBJECT TERMS. Key words or phrases identifying major concepts in the report.

16. SECURITY CLASSIFICATION. Enter security classification in accordance with security classification regulations, e.g. U, C, S, etc. If this form contains classified information, stamp classification level on the top and bottom of this page.

17. LIMITATION OF ABSTRACT. This block must be completed to assign a distribution limitation to the abstract. Enter UU (Unclassified Unlimited) or SAR (Same as Report). An entry in this block is necessary if the abstract is to be limited.

Ultrabroadband Phased-Array Receivers Based on Optical Techniques

Final Report by Dr. Christopher Schuetz and Brock Overmiller

To: gernot.pomrenke@afosr.af.mil
Subject: Final Report to Dr. Gernot Pomrenke
Contract: Ultrabroadband Phased-array Receivers Based on Optical Techniques
Contract #: FA9550-12-1-0380
Reporting Period: July 2012 –July 2015

Summary of Accomplishments:

Military operations require the ability to locate and identify electronic emissions in the battlefield environment. However, recent developments in RADAR and communications technology are making it harder to effectively identify these broadband and increasingly dynamic emissions. Consequently, our focus over the past three years has been to address the need for ultra-wideband detection and location based on optical techniques. In order to distinguish emitters in the scene, phased-array systems were investigated due to their relatively high-gain beam steering and nulling capabilities. We have addressed the need for electronic emission detection by developing a broadband imaging receiver for the location and identification of microwave and millimeter-wave emitters.

This approach utilizes photonic techniques to realize an imaging receiver that enables us to capture and convert signals across an array using photonic modulators, routing these signals to a central location using fiber optics, and spatially and spectrally processing the incoming signals using simple free space optics. To realize such an imaging receiver, a closed loop phase control system for the compensation of phase fluctuations induced on the optical fibers has been developed. Additionally, we have developed an optical heterodyne approach that utilizes an injection-locked optically-paired source to directly downconvert detected emissions for broadband signal recovery. Finally, methods were developed to simultaneously locate the source and emission frequency of signals within the scene using optical processing techniques that utilize chromatic effects of the array scaling and optical splitting of the signals, using a technique we refer to as "k-space processing."

Over the course of this effort, we have, for the first time demonstrated the capability of using such an optically enabled imaging receiver array to simultaneously detect, locate, and downconvert multiple high-gain beams in a non-blocking fashion using an optically enabled imaging receiver array. This technology was demonstrated first by adapting an existing 35 GHz passive millimeter wave imager that predated this effort, and then through the build of a four element broadband array, which is capable of detection over the range of 4-50 GHz.

Full Report of Stated Objectives and Accomplishments:

1 INTRODUCTION AND OVERVIEW

1.1 Introduction

One of the prime tenets in warfare is that of first knowledge, i.e. to be aware of your opponent before they are aware of you. In modern electronic warfare, this precipitates the development of increasingly capable RADAR, and on the flip side electronic support and intelligence systems. In the specific case of RADAR and counter-RADAR, systems meant to detect enemy sites typically have had a huge advantage over the RADAR systems they are detecting due to inherent disadvantage experienced by RADAR imposed by the two-way propagation required. This two-way propagation imposes path losses that decay as range to the fourth power, whereas typical RADAR detection systems have only a single path length and path losses from the RADAR decay as range squared. Practically speaking, this means that typical RADAR warning receivers and other electronic support systems have a detection advantage of power at the receiver that is typically many orders of magnitude larger than the power received by the threat RADAR. However, this power advantage is balanced against the fact that the RADAR transmits a known signal and can use matched filters to narrow the effective noise bandwidth of the receiver to the minimum level required to derive the information necessary for a given target. In contrast, electronic support system or RADAR warning receiver must open its received bandwidth to detect any threat possible in order to be effective. To date, search techniques based on known enemy RADAR profiles and relatively narrow transmitter bandwidths have swayed the balance largely in the favor of electronic support systems. However, the advent of modern wide bandwidth systems and reconfigurable electronics have enabled the ability to create extremely wideband and dynamic RADAR threats in which the power advantage experienced by RADAR warning receivers has largely been eliminated due to the need to increase receive bandwidths. Without reliable methods to predict and match the bandwidth of EW receivers to those of the RADAR they are detecting, such increases in receiver bandwidths, and with it receiver noise floors, are unavoidable.

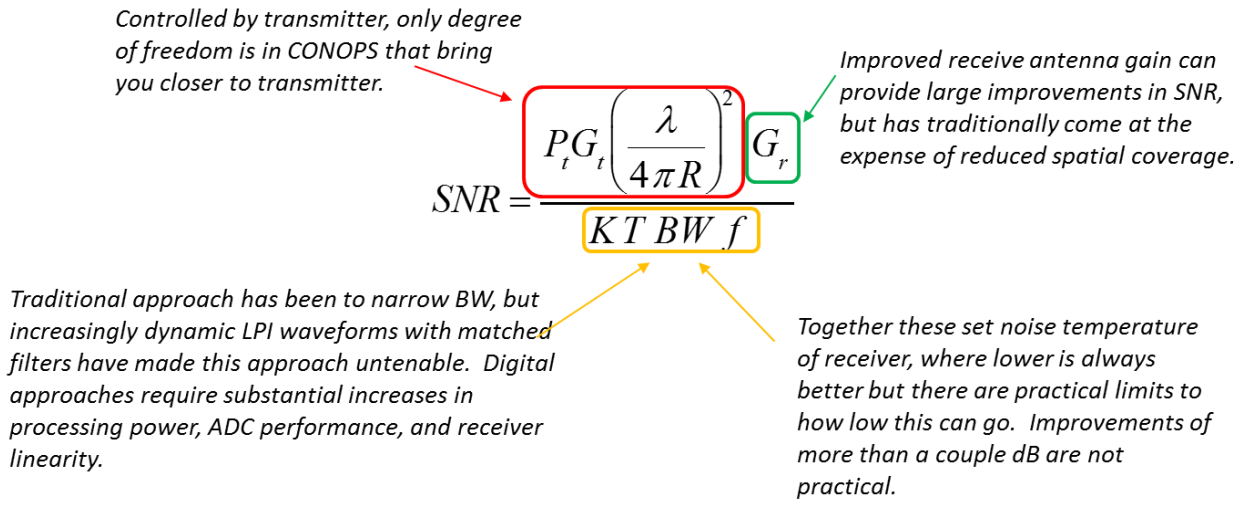

Figure 1. SNR of a thermally limited receiver based on Friis equation showing the limited degrees of freedom available in improving modern receivers.

To this end, a new approach is required to maintain the ability of electronic support receivers to detect RADAR threats without reducing the range required for detection, in order to keep platforms out of harm's way. As shown in Figure 1, the only significant degree of freedom left to modern receivers is to increase the effective gain of the RF receive antenna. In traditional systems, since gain and acceptance angle of antennas are inherently inversely related, this requires limiting the field of regard of the receiver. As such, the limited field of regard of the receiver either requires multiple antennas and receiver systems or must scan a single antenna, thereby lowering the probability of intercept of the signals of interest. Additionally, the high gain antenna structures are difficult to achieve without physically large steering gimbals which are not practical on most platforms. Phased array antennas could be utilized but are difficult to implement with more than one steering angle at a time, creating significant scan-on-scan problems, which significantly lower probability of intercept.

Under this effort, we explored a novel optically sampled phased array architecture which provides the benefits of a high gain phased array antenna, while simultaneously forming and sampling all of the possible beams that could be formed by that array using optical image forming techniques. The primary benefits of this approach are two-fold. First, the array provides the required increase in receiver antenna gain to maintain awareness of threats prior to impinging on their detection range. Secondly, the inherent direction finding of these imaging receivers provides spatial separation and location of various sources within the field of regard of the array, thereby sifting these signals based on spatial location, which is one of the few parameters of emerging threats that cannot be readily dynamically changed.

1.2 Imaging Receiver Architecture

Under this effort an EW receiver technology based on optical upconversion and processing was investigated. In this approach, the signals are collected via a distributed antenna array as shown in Fig. 2, and are then immediately converted into optical signals via broadband optical modulators. Subsequent routing and processing is completed in the optical domain using lightweight fiber optics and optical lenses. This approach provides a number of advantages over traditional receiver technologies. Of these, the primary advantage is that optical processing inherent to the approach separates received signals based on their AoA at an image plane in the receiver. In this manner, a simple CCD camera can be used to quickly map all incident energy in a broad frequency range based on the spatial position of the source. In addition, optical phase shifters inherent in the upconversion process can be utilized to steer energy from a particular AoA onto a high speed photodetector for further spectral and time based analysis as shown in Fig. 2(a). Such signals may even be mixed with an optical LO for direct conversion to baseband. In addition, such an approach has the added advantage of being low SWaP by virtue of the optical fiber, while still maintaining the ability to be integrated conformally to various platform architectures and can even be built around existing asset infrastructure without significant performance impacts.

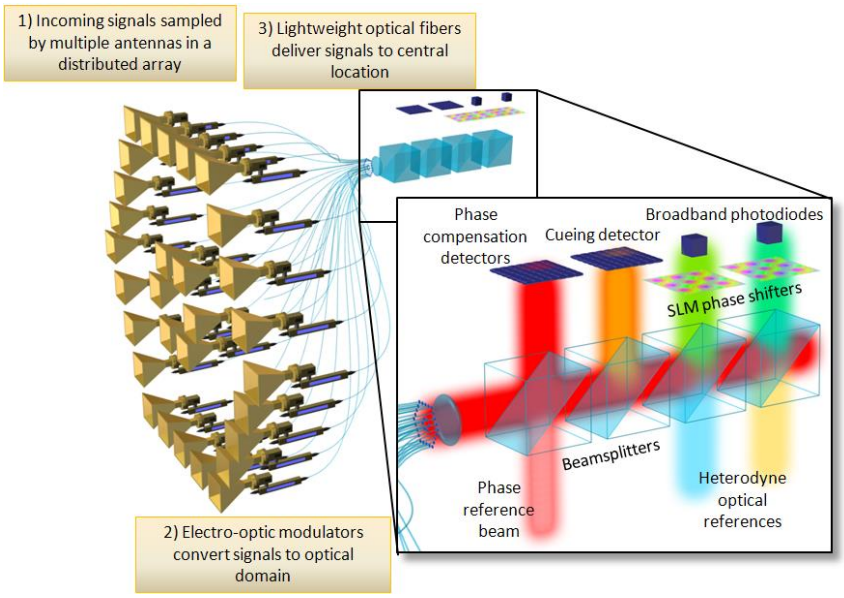

Figure 2.Optically enabled EW receiver concept.

Such an approach promises to yield extremely wide accessible bandwidths by virtue of the fact that optical processing is effectively narrowband and the bandwidth is limited only by the antenna and associated front end electronics prior to upconversion. The proposed receiver technology has been demonstrated in Ka-band as shown in Fig. 3(b). This proof of concept receiver demonstrated sufficient sensitivity for detection of passive levels of radiated emissions. This imagery is created in real-time using a simple optical camera. This same approach yields a high-sensitivity, broadband cueing receiver that can be paired with a high-speed photodetector as shown in Fig 3(a) for realization of a low CSWaP, broadband EW receiver.

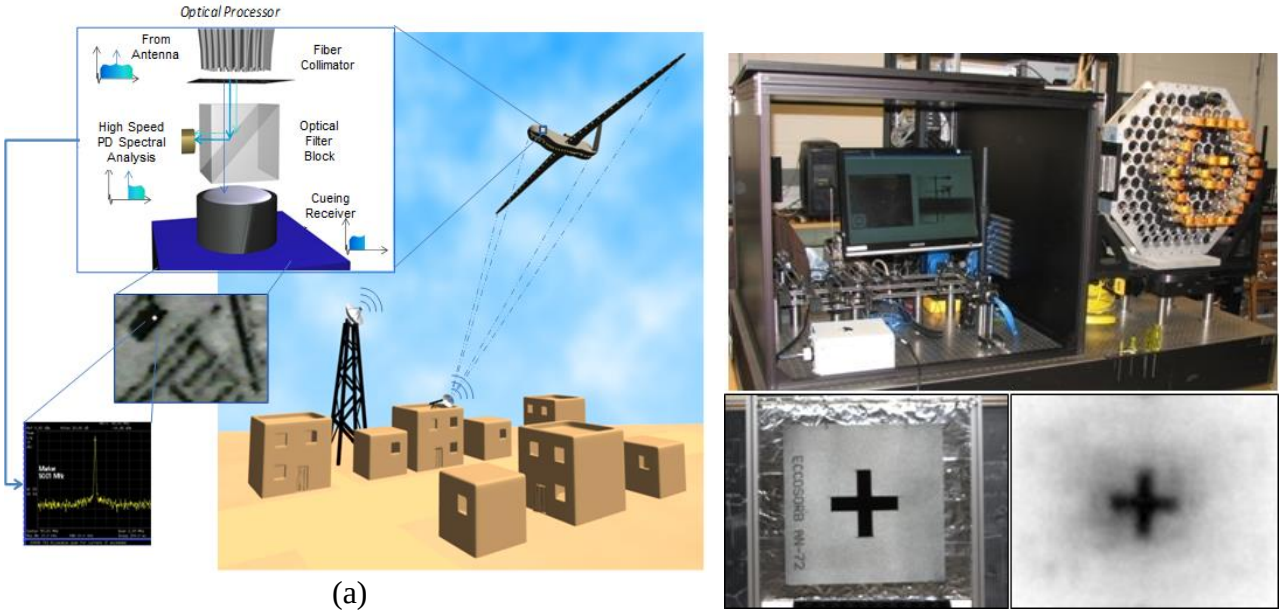

(a) (b)

Figure 3. Showing (a)conceptual realization of cueing receiver with capabilities for spectral and temporal signal identification and (b)experimentally demonstrated optically enabled receiver with sufficient sensitivity for capturing passive radiometric image shown in bottom right.

The proposed approach has several advantages over traditional receiver systems. These advantages include:

- Low-loss, dispersionless routing of **multi-octave signals** using optical fiber
- Differentiation and separation of signals from varied spatial locations (spatial decomposition) based on processing of angle of arrival using simple, compact free-space optical techniques
- Spectral decomposition by heterodyning with an optical local oscillator (LO) to bring the signal directly to baseband—ready to be digitized for further processing in the electronic domain
- Easy **expandability to a large number of antenna channels** as all channels are processed using common free-space optics
- Reception of **multiple independently steered beams**
- Easy expandability of the number of received beams that can be implemented using a common front end simply though the placement of additional photoreceiver assemblies
- Phase control of each channel that allows setting **independent direction of receive beams** of the array for each receiver element

Successful realization of such a receiver topology could provide a new paradigm for broadband, multifunctional receivers.

Under this program, the following specific tasks were undertaken to prove the viability of these concepts towards yielding a new class of electronic support receivers.

1) Imaging Receiver Proof-of-Concept - An existing optical receiver array fabricated for passive millimeter-wave imaging at 35 ± 2 GHz was modified to demonstrate the recovery of active RF signals within the array field of regard. Viability of concept was demonstrated, but sensitivity was limited by difficulties coupling the free space optical signals into the fiber coupled optical detectors necessary to recover signals at these frequencies.
2) Optical Downconversion Proof-of-Concept - An injection-locked optical paired source was created which enabled the direct heterodyne of RF signals to baseband in the optical domain. Operation of this paired source was demonstrated in conjunction with the imaging receiver and several sample system demonstration concepts were developed.
3) Trade Study Comparison - Trade studies were completed in conjunction with another AFRL effort to investigate the utility of this technology against traditional EW receivers. Key findings were incorporated into a notional system design and specifications for this notional system were compared against a modern public RADAR warning receiver specification.
4) Channel Integration Efforts - Investigations into new techniques for RF and photonic integration based on liquid crystal polymer substrates were pursued that would aid in the realization of potential imaging receiver designs.
5) New Concepts Developed for Achieving Extending Frequency Range – A broadband receiver was designed and built that utilized optical carrier rejection in a low biased Mach-Zehnder modulator to suppress the optical carrier and extend the low end of the frequency of operation of the imaging receiver technique. Operation of this receiver from 4- 40 GHz has been demonstrated.

Each of these tasks is discussed in the following sections respectively.

2 IMAGING RECEIVER PROOF-OF-CONCEPT

To provide the optimal benefit on this research effort, the PI was able to leverage an existing hardware base, built as a proof-of-concept passive millimeter-wave imager. In this section, we describe the imager used as a base and the modifications made to it to enable spatially resolved signal recovery.

2.1 Pathfinder Imaging Array

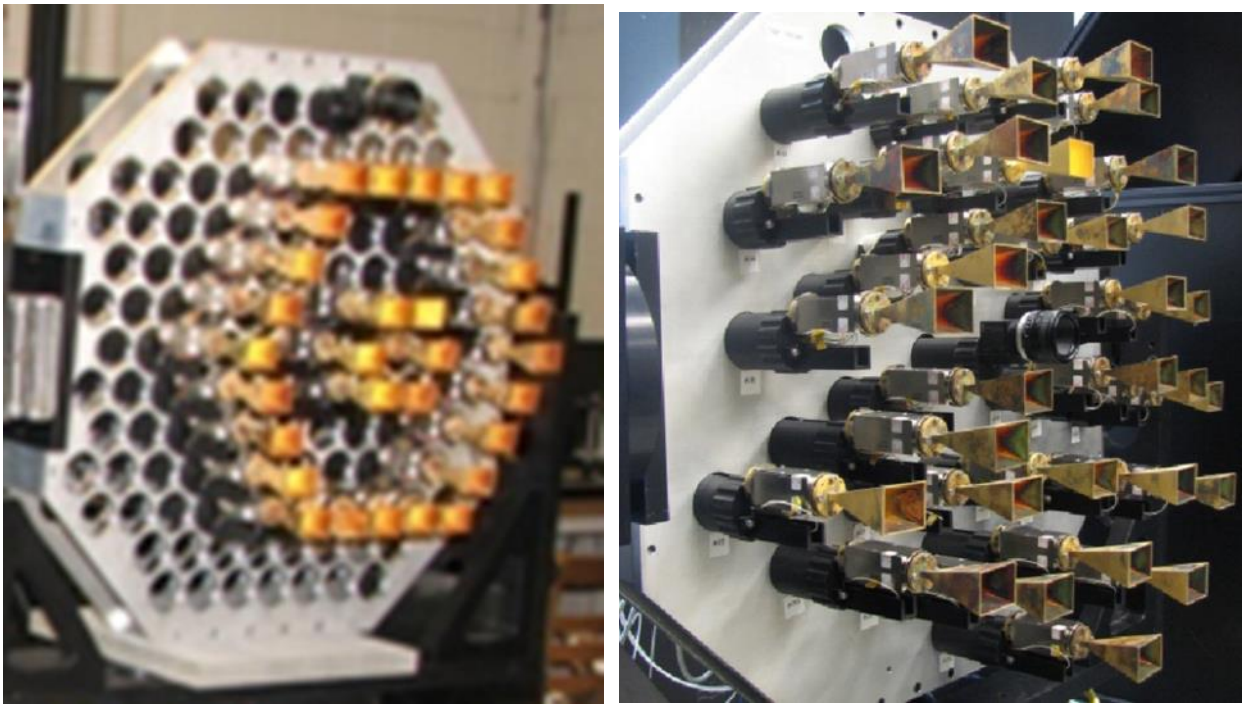

Figure 4. Pathfinder I (periodic) antenna array (left) and Pathfinder II (aperiodic) antenna array (right).

As a starting point for this effort, the PI had access to a previously built passive millimeter-wave (pmmW) imager that utilized the optical upconversion techniques that are at the core of the proposed EW receiver approach. This pmmW imager, dubbed Pathfinder, consists of a 30-channel, 35- GHz imaging array built of commercially available components. The imager was built first as a sparse array on a regular grid and then later upgraded to an aperiodic array as shown in Figure 4. Various aspects of the hardware implementation of the array used for these tests are shown in Figure 5. Additionally, the layout of the optical processor, which provides for both phase control and compensation of the optical channels as well as the optical filtering and formation of the spatial Fourier transform of the fiber array for image recovery, is shown in Figure 6. The aperiodic array was chosen for passive imaging in order to minimize the presence of grating lobes due to the sparsity of the array. The aperiodic structure blurs the grating lobes of the array, which mitigates "ghost" image formation in passive images. For the purposes of this program, where the imaging receiver is to be used as an EW receiver, the sparsity of the array and the resulting sidelobes in the point spread function serve as a limiter on the ability to spatially reject signals. Sidelobes in the point spread function (PSF), which can be readily calculated by taking the spatial Fourier transform of the positions of the antennas in the

array, result in signal from other parts of the image being mapped across the array according to the strength of the sidelobes.

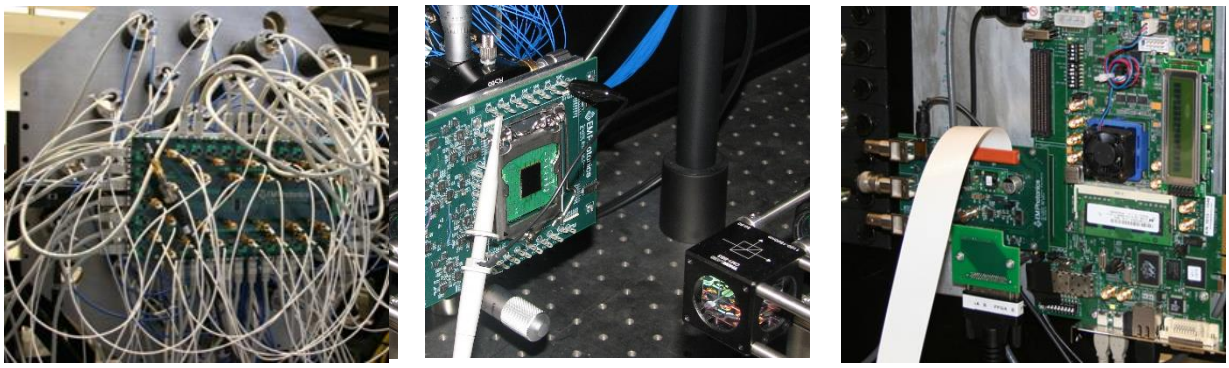

Figure 5. Power Distribution attached to antenna array (left), FPA Receiver Board (middle), and FPGA Board (right).

A representation of these sidelobes and their effects for the Pathfinder array configuration are shown in Figure 7. For the aperiodic Pathfinder configuration chosen for passive imaging, the thirty channel array demonstrates a maximum sidelobe level of ~20%, or 7 dB, with an average sidelobe level of ~3%, or 15dB, over the extent of the 20° field of view set by the gain of the individual antenna elements. Due to the sparsity of the array, the percentage of total power present in the main beam, or diffraction efficiency, was only ~8% for this array. The remaining power is spread amongst the sidelobes as dictated by the PSF, resulting in signals from one direction mapping to a lesser extent into other parts of the image.

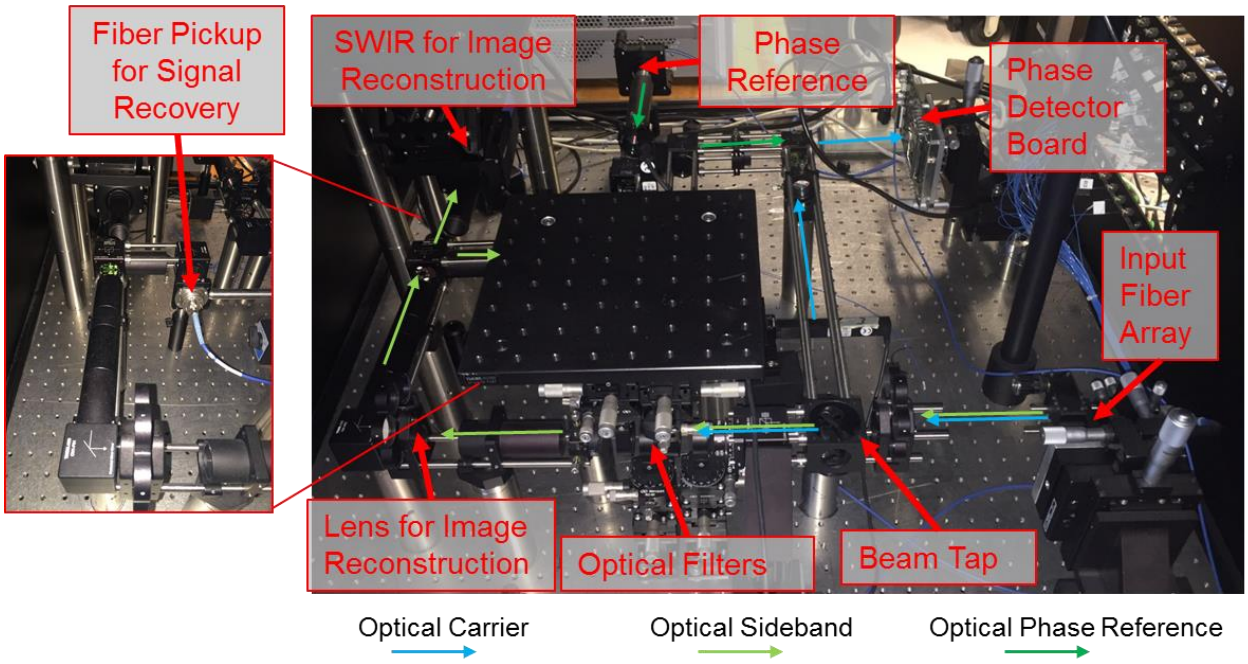

Figure 6. Optical processor for Pathfinder imager modified to include fiber pickup for signal recovery.

While this low diffraction efficiency is hardly desirable from the perspective of electronic receiver, where we are trying to isolate signals from one another for analysis, it was dictated by the fact that the array was primarily designed for pmmW imaging applications, where the fundamental trade between field of view (dictated by the size and directivity of the individual array elements), resolution (dictated by the physical extent of the array aperture), and cost (dictated by the total number of elements in the array and thus determining fill factor) must be traded. Thus, for a pmmW imaging standpoint a sparse array is often indicated to optimize resolution and fill factor while lowering cost of the array. This tradespace when revisited for electronic warfare applications would place a greater emphasis on effective spatial separation of signals over precision of spatial location (resolution) and therefore densely packed arrays would be indicated for most electronic warfare receivers. Nonetheless, the hardware shown in the Pathfinder array, while not optimal, provided an excellent starting base for the proof of concept of many of the techniques pursued by the program and allowed us demonstrate in hardware many concepts that the PI would otherwise not have had the resources to demonstrate under this effort.

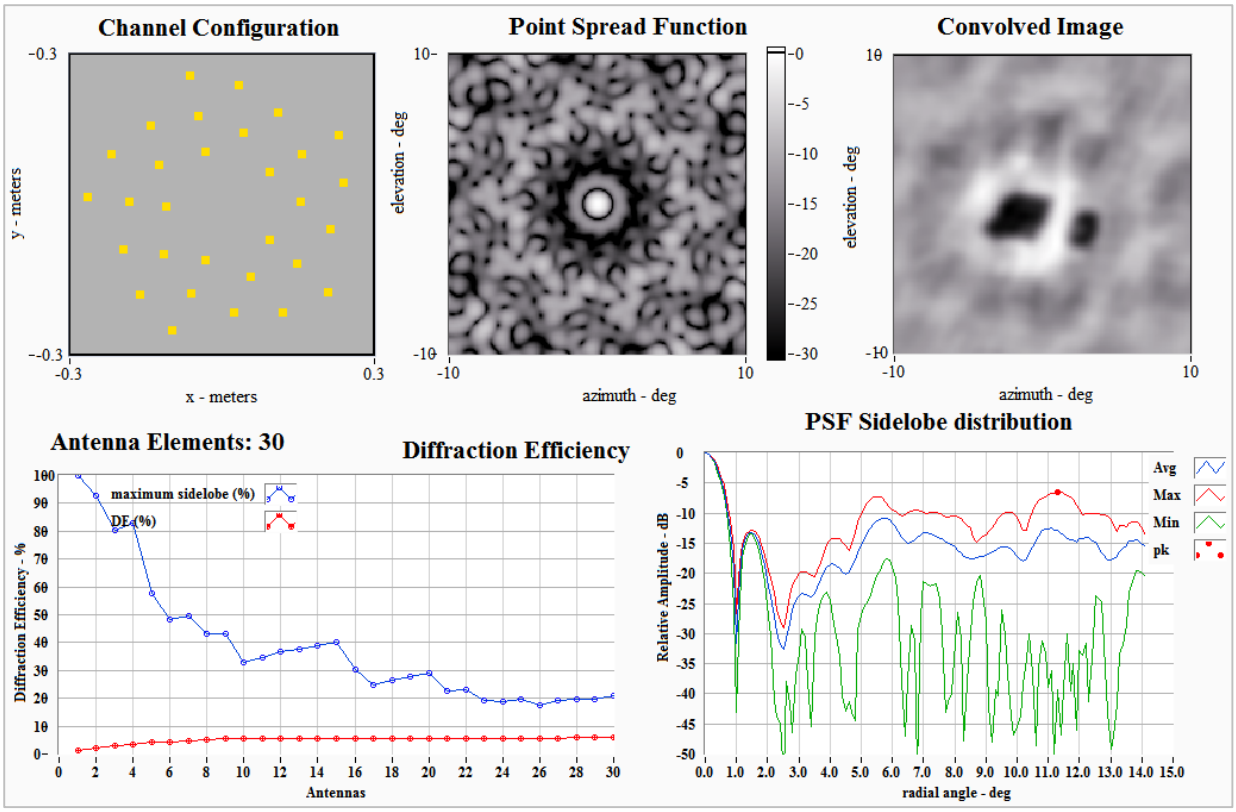

Figure 7. Showing spatial layout of the antenna positions in the Pathfinder array (top left) and the corresponding PSF of that array on a log intensity scale (top middle). The passive image of a tank and a truck at a range of 50m is also shown (top right). The maximum, average, and minimum sidelobe levels as a function of angle from the center of the PSF on a log scale (bottom right). Finally, the maximum sidelobe level and diffraction efficiency , or amount of energy falling in the main beam of the PSF, are shown as a function of number of elements in the array for a random population order of the array configuration shown (bottom left).

The main impact of this configuration for EW applications is that the ability to reject signals outside of the primary spatial direction being sampled is limited to the maximum sidelobe level present in the direction of that signal. For most EW applications, the optimal array configuration would be a densely packed array, in which sidelobes can be largely eliminated (sidelobes less than 30 dB across the field of regard should be readily achievable). Such dense arrays are trading away aperture size and thus apparent resolution for a given number of elements. However, for electronic warfare applications, where the goal is to detect active emissions, dense arrays provide equivalent sensitivity to sparse arrays while improving the ability to reject signals from other locations.

Since we were leveraging this existing hardware to accomplish much of the testing for this program, we were somewhat limited in the modifications that could be made given the resources of this effort. To this end, we focused on modifications that would enable the signal recovery and downconversion of the detected signals, as described in the following sections.

2.2 Optical Processor Modifications for Signals Recovery

One of the primary goals of this program was to demonstrate spatial decomposition of the received signals, whereby spatially separated electronic emissions never impinge on the same detector, and hence intermodulation spurs are mitigated unless sources are co-located. Figure 8 illustrates the approach as initially proposed.

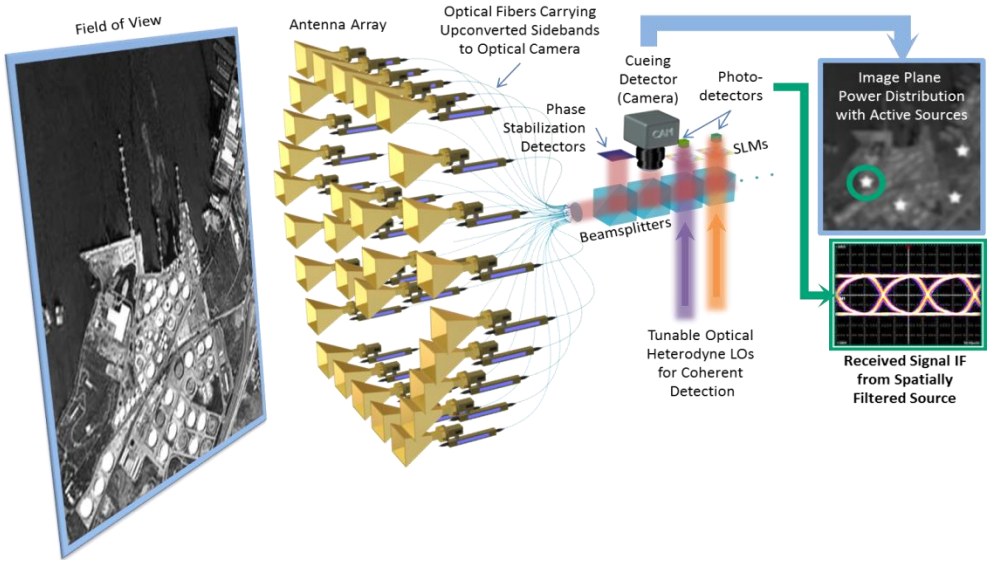

Figure 8. Illustration of the ability of the proposed architecture to improve the receiver's effective linearity. Spatially separate RF sources are isolated and separately tracked in the image plane (top right), and spatial light modulators (SLMs) are used.

Within our imaging receiver's optical processor, several functions are performed in order for the emissions to be properly detected and analyzed. First, the conversion to optical wavelengths makes the routing sensitive to phase fluctuations on the order of an optical wavelength. Thus, an active

compensation mechanism for vibration and thermal variations is required to stabilize the phases on each channel. Once phase stabilization is completed, one of the sidebands is passed to a cueing detector. This is accomplished using simple optics to perform a spatial Fourier transform of the overlaid sidebands to resolve an image of the collected RF radiation. This concept has been used to build an imaging array with sufficient sensitivity to image passive radiometric emission which can be seen in the following section. All of these capabilities were present in the hardware at the start of this effort.

One of the key developments proposed and realized in this program was that upon detection of RF radiation by the cueing detector, the same optical processor can be used to identify the resolved signals. The optically upconverted RF radiation is sent through a 3 dB optical beam splitter before the cueing detector and relayed to an optical recovery port. This recovery is accomplished by combining the resolved emissions spot with the original carrier offset to quadrature phase to recover the signal on a high speed photodiode. The port was designed to correspond to the center of the cueing detector as well as encompass the entire field of view (FOV) of the receiver. These sources are then routed onto a high-speed photodiode and can potentially be mixed with a coherent optical heterodyne LO for RF signal recovery. A description of the technology used to generate the optical LOs can be found later in this report.

To accomplish these modifications to the system, several techniques were attempted for optically coupling to the high-speed photodiode for signal recovery. Since the imager works by filtering the optical carrier from the sidebands prior to image formation, provisions had to be made to recombine the optical carrier or an offset optical carrier for downconversion as described in section 3. Initial effort to establish the carrier recombination in free space caused degradation in the cuing receiver imagery due to the relatively high light levels of the carrier to sideband causing scattering and backreflections in the optical path to overwhelm the sideband imaged on the SWIR camera. To mitigate these effects, a lenslet based fiber coupler was placed after a beamsplitter in the optical path as shown in Figure 6. Using this fiber coupler allowed the carrier to be combined using a simple 3dB fiber splitter/combiner and allowed for testing of different techniques. However, the fiber coupler provided one significant drawback in that significant coupling loss (>20 dB) was introduced by the fiber coupling that placed significant limits on the sensitivity of the signal recovery that could be achieved by this fiber pickup. This source of loss was only recently discovered to be a limiting factor in the system sensitivity and plans are being developed to replace this coupler with a direct free space coupling into a photodiode using optical isolators to mitigate effects of optical carrier reflection into the cueing detector.

2.3 Experimental Results

For initial experimental validation of the concept, we simply wanted to show that the imaging receiver was capable of both spatially identifying a signal and simultaneously identifying its frequency of operation. For initial characterization and identification, we required a source that operates around the

same frequency of the imaging system for proper detection. Mechanically tuned gunn diodes were chosen to act as our electronic emissions.

Figure 9 (left) depicts a millimeter-wave image including both the passive and active field of view. To passively image, our system detects the blackbody radiation given off by objects. Blackbody radiation contains the temperature information of each point in the scene. The greater the temperature differences in the scene, the more distinct passive objects become in the millimeter-wave image. In order to replicate the radiometrically cold sky (greatest temperature difference experienced outdoors) in a lab, liquid nitrogen (LN) was used. Liquid nitrogen is evident on the left side of Figure 9 (left) where black represents cold temperatures. Placed to the right of the liquid nitrogen was one of the 35 GHz gunn diodes to act as an electronic emitter. Both the liquid nitrogen and the gunn diode source were stationed three meters from the imager. Simultaneous imaging and detection on an electrical spectrum analyzer (ESA) for frequency identification occurred. Figure 9 (right) illustrates the spectra of bright spot in the image which originates from the emission from the gunn oscillator.

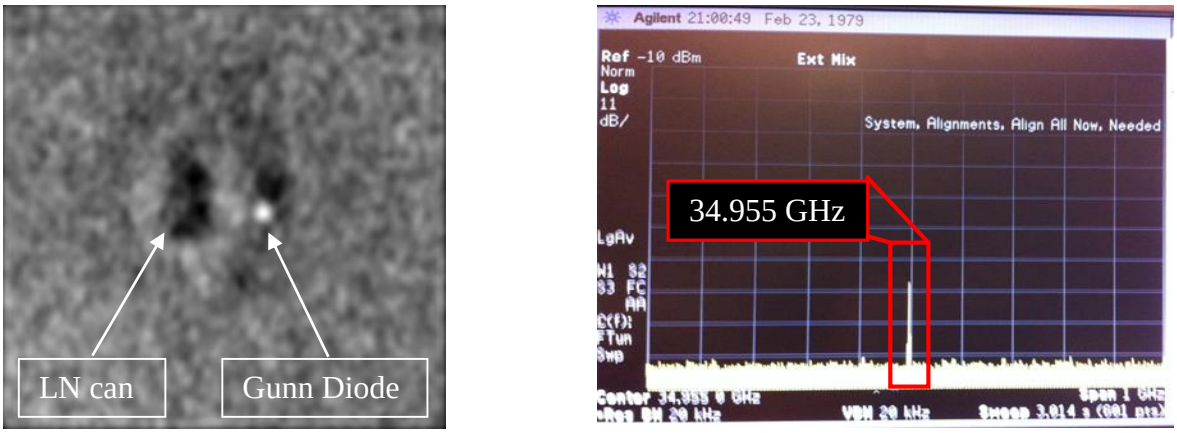

Figure 9. Image from 35 GHz passive millimeter-wave imaging system showing both passive and active field of views from three meters away (left) and the Mechanically tuned Gunn diode detected on an electrical spectrum analyzer (right)

Single source detection is very important on the electronic battlefield. However, in most practical cases, more than one source will be evident within one's field of view. This requires the ability to detect more than just a single source on the photodetector. To prove this capability, we placed two gunn diodes in the imaging scene to demonstrate the possibility of having multiple emissions within a field of view. Figure 10 shows the experimental setup, as well as the RF Spectrum Analyzer data, which proves that this imaging technique can detect more than a single source in one's field of view and identify the position on the cueing detector where it is emanating from. Currently, work is being done to optimize photodetection of received signals to ensure correct power distribution. See section 1.4 for quantitative results of power distribution through phase sweeps in the azimuth and elevation directions.

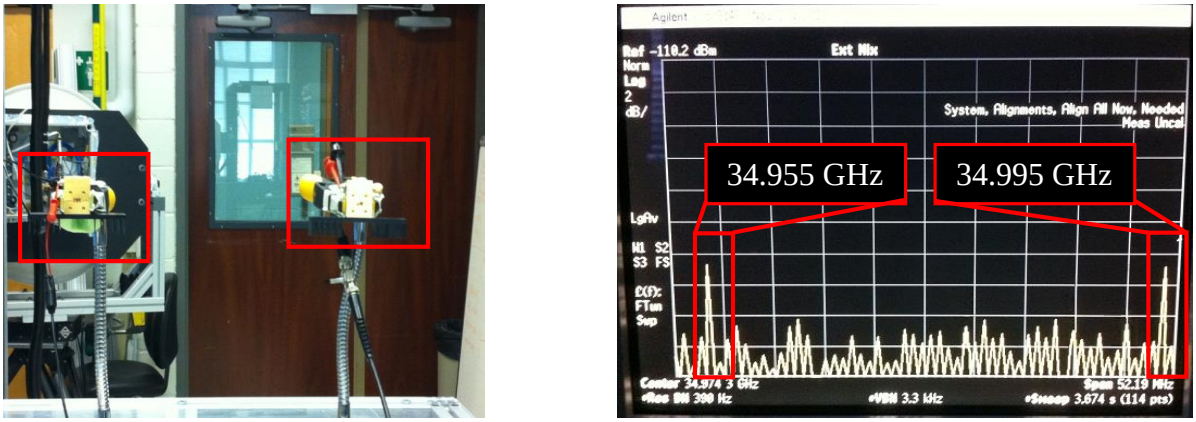

Figure 10. Image of two Gunn diodes in the imaging system FOV (left) and the RF Spectrum Analyzer recognizing both emitters (right)

To demonstrate the full capability of this photonic architecture, we added a beamsplitter to direct a copy of the image plane toward a 40-GHz high-speed photodiode, as indicated in the schematic of Figure 11. By applying appropriate phase shifts to the output of each modulator in the array, we have successfully shown that the image can be steered to a chosen position of interest (POI) onto the detector. The spectra shown in Figure 10 were both obtained with the detector in the same position, with no mechanical movement of any part of the system.

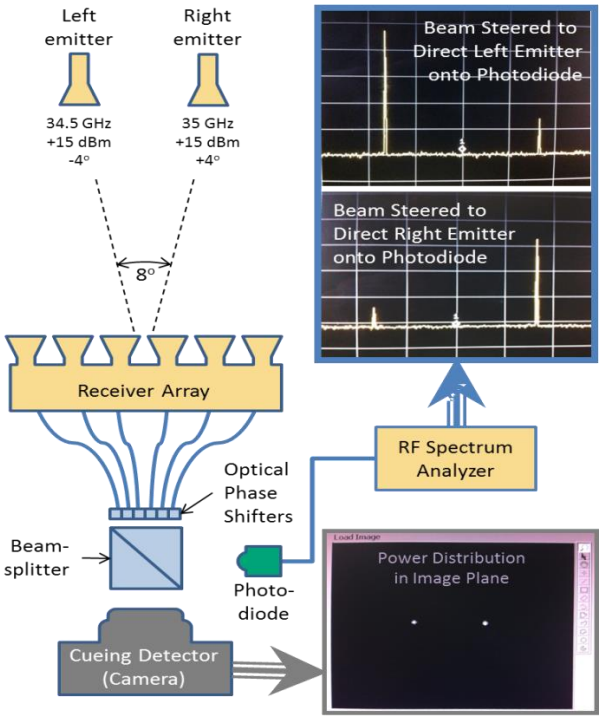

Figure 11. Illustration of a preliminary demonstration of spatial source discrimination by the proposed receiver configuration

Although this demonstration of signal recovery at baseband showed the promise of using this technique as an imaging receiver, the direct recovery of signals at baseband incurs some significant limitations. First, to respond at millimeter-wave frequencies, photodiodes must have small active areas. This limits the photocurrent that they can handle and correspondingly decreases the dynamic range and noise performance of the imaging receiver. The small photodiodes also complicate the coupling of the reimaged optical spot to the photodiode, thereby incurring losses in coupling to the photodiode either using fiber based optical couplers or direct free space coupling to the photodiodes. Additionally, direct signal recovery at baseband is not often necessary, since electrical technologies to digitize and process high dynamic range signals to the digital domain is limited by the analog to digital converters to ~1 Gs/s and downconversion to lower frequencies is required anyway. To this end, we have developed a technique for the generation and mixing of the spatially separated image with an offset injection locked optical carrier that provides direct downconversion of the received signals upon photodetection. This approach allows the use of lower speed photodiodes that are both easier to couple to and can handle higher power operation for improved dynamic range and noise performance. This technique is discussed in more detail in the following section.

3 DEVELOPMENT OF AN INJECTION-LOCKED OPTICAL SOURCE FOR PHOTONIC HETERODYNE DETECTION

3.1 Ultra-wideband Phased-array Receiver based on Optical Paired Sources

In the context of the receiver array architecture of Figure 8, a single (master) laser is amplified and split into 32 fibers. As stated above, 30 of the fibers are used as the inputs to the electro-optic modulators. One of the two unused fibers will be used to generate the coherent heterodyne optical local oscillators (LOs) according to the scheme shown in Figure 12 (top) and described below. As depicted in Figure 8, beamsplitters and spatial light modulators (SLMs) will then be used to direct spatially filter signals from their respective positions in the image plane onto photodiodes for heterodyne detection. The optical LO generation technology is based on modulation-sideband injection locking of semiconductor lasers, offering enormous bandwidth, superb signal purity via cancellation of optical phase noise, and size, weight, and power (SWaP) improvement due to the use of optical fibers and photonic components.

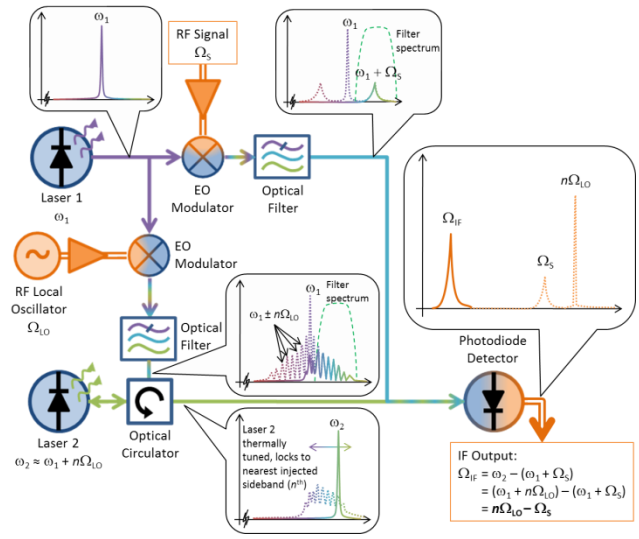

System Property	Preliminary Test Result	Projected Performance*
Input Signal Range	2–20 GHz	~2–200 GHz
Signal Bandwidth	4 GHz	Up to 10 GHz
IF	6.2 GHz	3-15 GHz
Gain	–25 dB	Up to 15 dB
Noise Figure	33 dB	15 dB
SFDR (in 1-Hz BW)	~100 dB	125 dB

*based on 10-V V_π & 500-mA I_{DC}

Figure 12. Single-channel photonic receiver. In the proposed effort, this scheme would be used to generate coherent optical heterodyne LOs (top) and Table of measured and projected performance for this system (bottom)

Our initial implementation of this concept is a widely tunable RF/millimeter-wave (mmW) source, which generates ultra-pure RF carrier signals by photomixing injection-locked lasers on a high-speed photodiode (PD). Wide tunability is realized by injection locking using a broad comb of sideband harmonics, all derived from externally modulating one laser with a low-frequency RF reference that has been subject to nonlinear distortion through RF amplification. The second laser, or slave laser, is then thermally tuned to match and lock to the frequency of any one of the injected harmonic sidebands. Choosing higher harmonics allows very high offset frequencies to be obtained and because the locked lasers have identical phase noise, the purity of the reference is preserved. Demonstrations have been conducted showing continuous tuning over 7 octaves (0.5-110 GHz), with a measured linewidth of ~1 Hz over that entire range. The method of wide-band EW detection may be able to span the entire millimeter-wave range (30-300 GHz) with UD-developed modulator technology.

With a small modification, the system can function as an ultra-wideband photonic tuner (figure 9 (a)), enabling RF-mmW signals to be received and processed with exceptional instantaneous bandwidth (IBW) and spur free dynamic range (SFDR). By coupling the RF receiver design in the path (Figure 12 (top right)) of the master laser (Laser 1), we get a received optical signal $\omega + \Omega_s$ on the recovery port with significant bandwidth. The injection-locking scheme is then used to generate an optical LO,

whose frequency offset from the optical master laser is chosen so as to downconvert the received signal to a desired IF (i.e. baseband frequency range), where it can be captured by a photodiode. Notably, the photodiode need only possess sufficient speed for the IF plus the signal bandwidth, not the RF carrier frequency, so the tuning range of the tuner is not photodiode limited, and can extend to the full range of the modulator's operation. This feature allows us to use photodiodes with higher optical power handling and output photocurrents.

3.2 Optical local oscillator

The proposed ultra-wideband photonic downconverter illustrated in figure 9 (a) has been constructed and implemented into our imaging receiver. The concept is to take the spatially resolved signal from the imaging system as seen in Figure 13 and combine it with an optical local oscillator (LO) to generate a desired IF as stated above. In Figure 13 (left) an RF source is set 2 meters away from the antenna array, upconverted to an optical wavelength, and sent to our central processor for filtering, phase compensation, and detection on the cueing detector as shown on the monitor (bright RF spot).

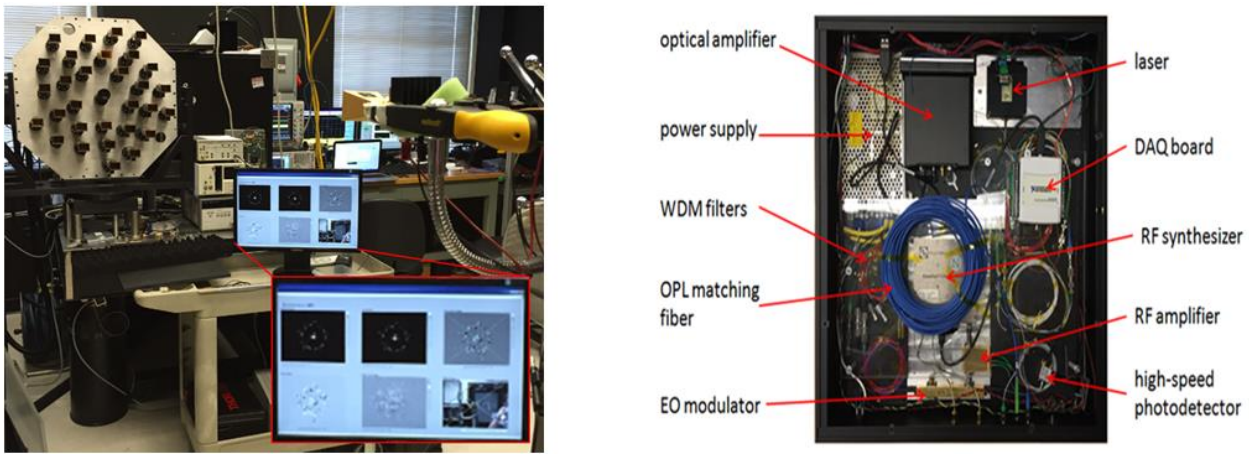

Figure 13. The imaging receiver detecting an RF emission 2 meters away (left), and the designed optical local oscillator design with components labeled (right)

Figure 13 (right) displays the designed optical LO. As stated above, one of the 32 fibers from the master laser is sent into an electro-optic modulator that is subject to nonlinear distortion. The output of the modulator is sent to 100 GHz WDM filters to filter out the optical carrier as well as the lower portion of the optical sidebands as they are unused. The non-filtered upper sidebands are sent to a booster optical amplifier for appropriate injection-locking. The amplified signals are injected into our slave laser. The laser does not have an isolator, allowing signals to inject themselves into its cavity. The slave laser is then thermally tuned by altering the voltage of the DAQ board to change the wavelength emission to the desired harmonic frequency. Once locked to the desired harmonic, the slave laser is mixed with the recovered signal from the EW receiver and combined onto a

photodetector. The recovered signal is sent through an optical path length (OPL) match fiber to match the path lengths of both arms, essentially reducing the phase noise and reducing the linewidth of the RF generated signal.

Initial tests proved accurate detection and down conversion of received RF signals. In one case, a 35 GHz signal was emitted in free space aimed at the imaging receiver. To fully grasp the capability of the system, the optical LO was locked to the 5^{th} harmonic of 6 GHz off of the master laser. With the RF radiation set to 35 GHz and the LO set at 30 GHz, a 5 GHz signal was expected on an RF Spectrum Analyzer after mixing on a high-speed photodetector. When connected to the spectrum analyzer, a 5 GHz was realized as shown in Figure 14.

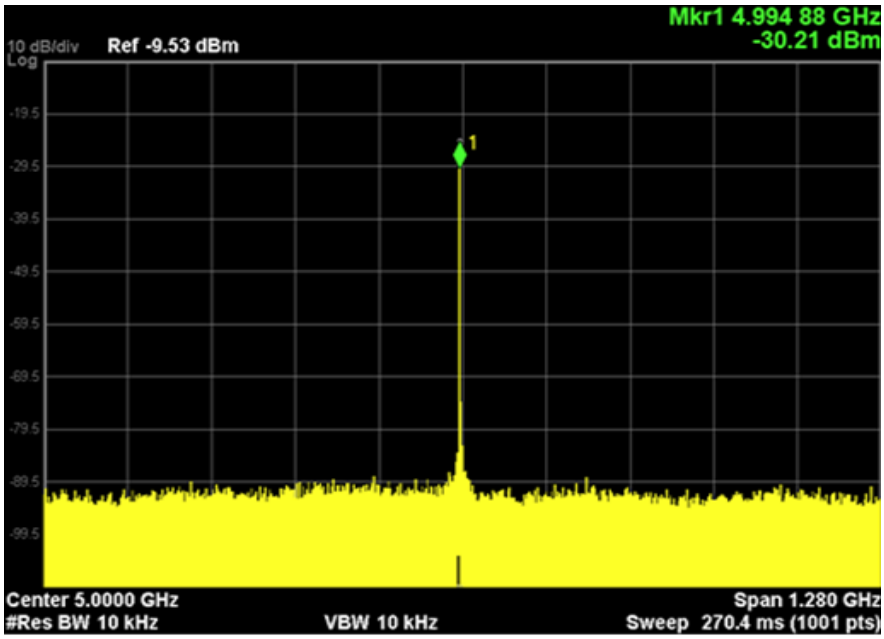

Figure 14. Downconverted RF radiation from 35 GHz down to 5 GHz using an optical LO approach

3.3 Recovering Modulated Signals

The concept of downconverting incoming RF emissions was extended to signals containing modulated information, such as music or a tone. In an effort to properly characterize our imager for threat suppression and signal recovery, we developed a photonic tuner demonstration setup. The setup used two transmitters, a music/tone transmitter, and a jammer/siren transmitter. The two transmitters can be seen in Figure 15 (left) 2 meters away from the imaging receiver as well as the spatially separated spots on the cueing detector in Figure 15 (right).

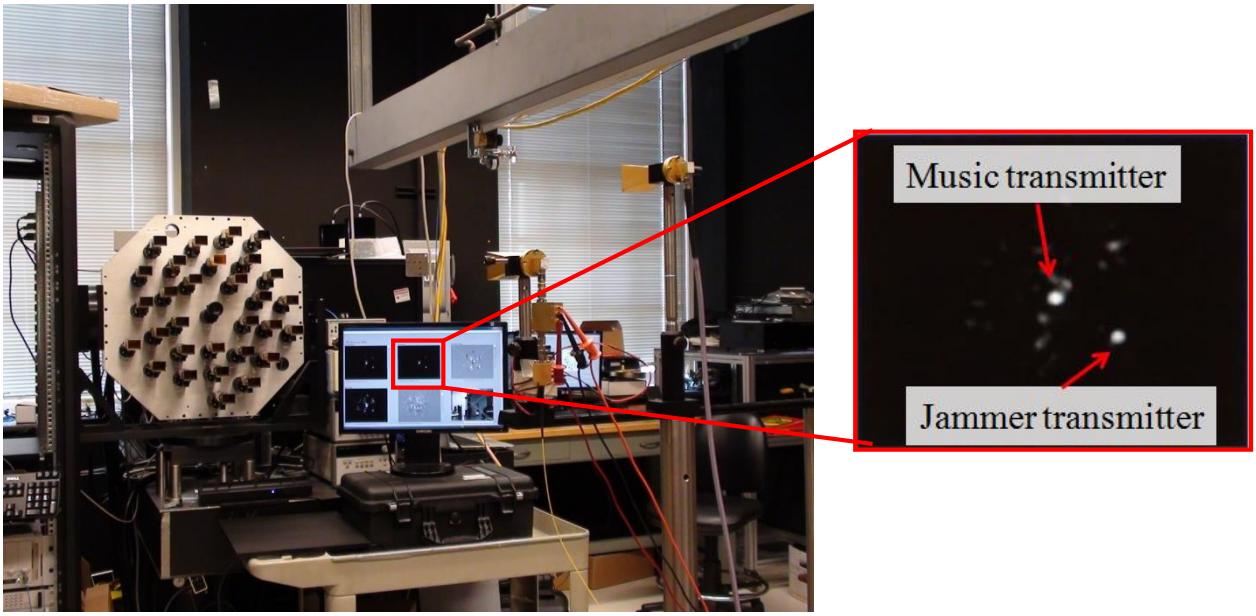

Figure 15. Two Tone receiver setup with the imaging receiver beam steered toward the music transmitter (left) and the cueing detector image of the two sources with the music transmitter centered on the image (right)

A schematic of the photonic tuner downconverter is illustrated in Figure 16 (top). As described in earlier sections, the master laser is split to both the imaging system and the LO. The modulated RF is received by the imaging system and beam steered onto the signal of interest. By beam steering to the signal of interest, the music RF spot seen in Figure 16 (top) illuminates the recovery port whereas the jammer signal is suppressed below detectable levels. The LO is set to 35 GHz offset from the master laser. With the transmitters set to the same frequency, 35.01 GHz, this corresponds to a 10 MHz IF on the photodiode. The generated downconverted signal is then relayed to an RF Spectrum Analyzer for processing. Figure 16 (bottom) shows the IF signal at 10 MHz with the music transmitter's instantaneous bandwidth and modulated tone. It is evident in Figure 16 (bottom) that the only signal recognized and recovered in the music tone as the unwanted jammer signal is suppressed.

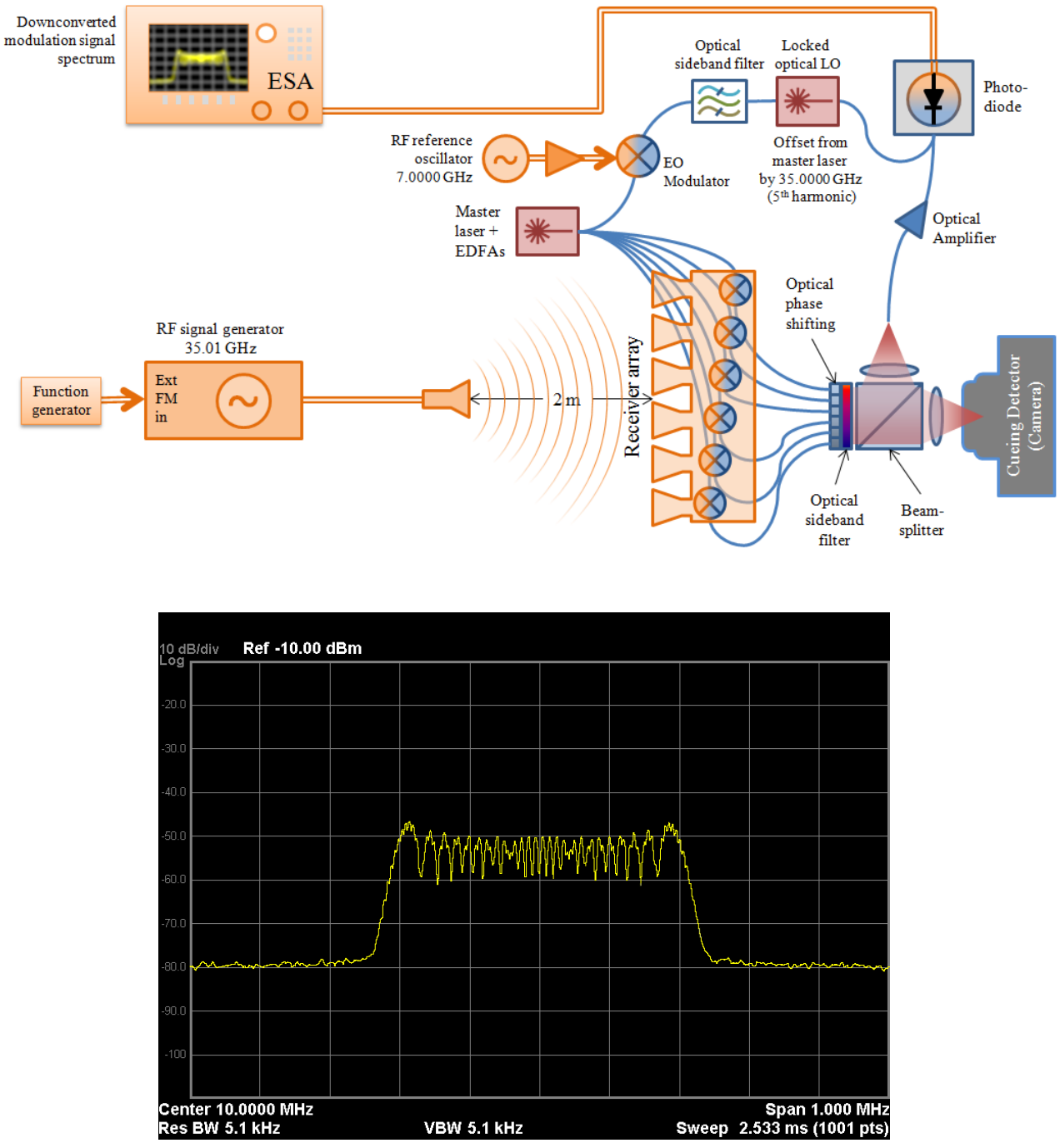

Figure 16. Photonic Downconversion Demonstration Setup with an audio tone transmitting on a 35.01 GHz RF carrier (top) and the recovered signal at a 10 MHz Intermediate Frequency (bottom)

More recently we have demonstrated the use of this imaging receiver technology to recover and downconvert complex modulated digital communications signals, with spatial suppression of co-channel interference as shown in Figure 17. In this demonstration, a 35.295 GHz carrier signal was

encoded with 16-QAM data at a symbol rate of 10 Ms/s and launched into free space with a standard 20 dB gain horn with a transmission power of ~0 dBm. A second unmodulated transmitter was placed at a separation of ~4 inches with an identical transmission power and emission frequency providing a strong source of co-channel interference. The QAM signal, when recovered using a single 20 dB standard gain horn at a range of 1.7m through downconversion on a Keysight PXA spectrum analyzer, was recoverable with acceptable SNR(>20 dB) only when the co-channel interference was not present. Using the imaging receiver, the same QAM signal was recovered showing comparable SNR when the co-channel interference (CCI) source was turned off. When the CCI source was turned on the imaging receiver received little to no degradation in SNR, while the signal recovered by the single standard gain horn degraded by more than 15 dB, making digital signal recovery unfeasible.

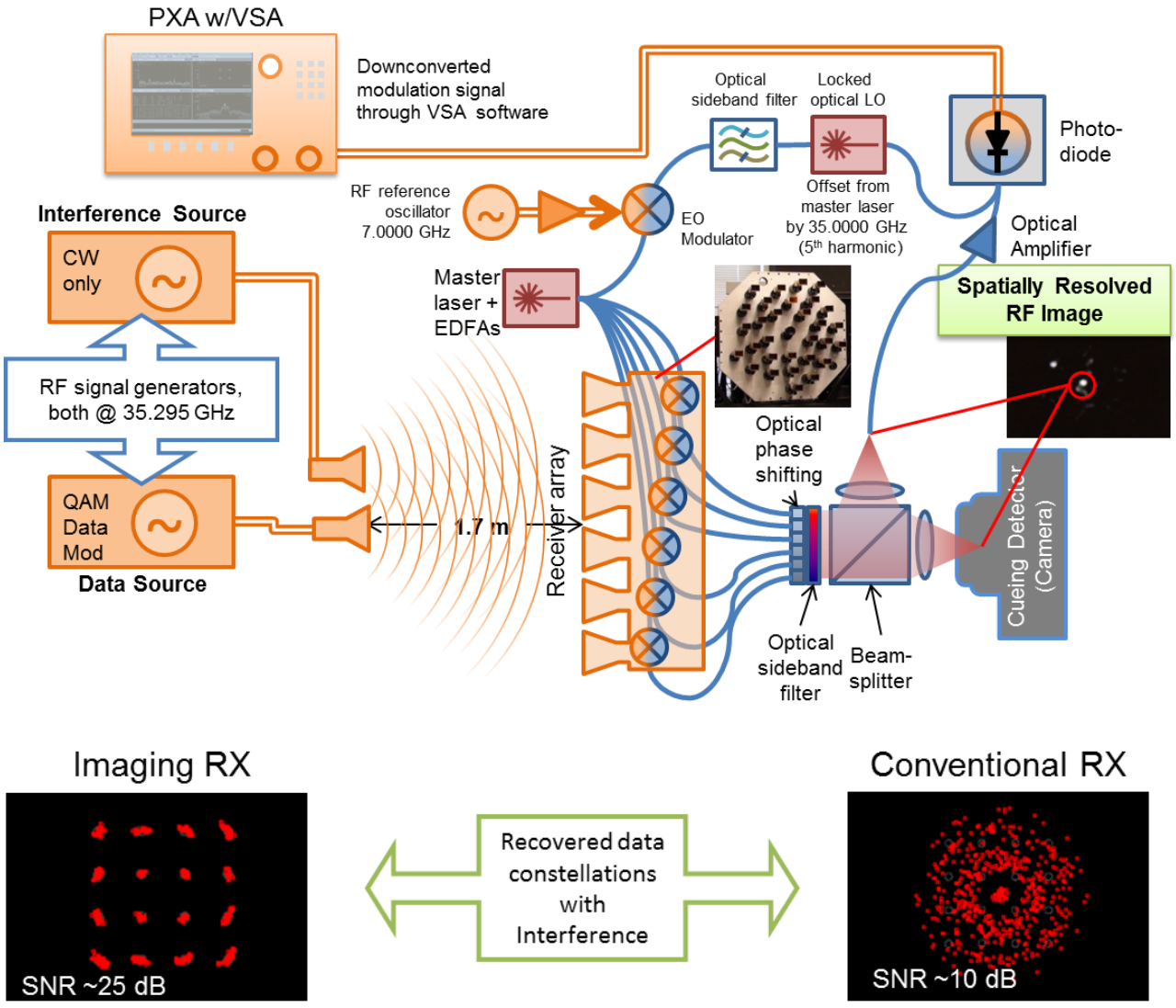

Figure 17. Photonic downconversion demonstration of communications signal recovery in the presence of co-channel interference.

4 EW TRADE STUDIES

As part of this effort, the PI participated in a series of trade studies evaluating the efficacy of using the proposed photonically sampled antenna arrays for application as an electronic warfare receiver. Existing Electronic Intelligence (ELINT), Electronic Support (ES), and RADAR Warning Receivers (RWR) are having an increasingly difficult time identifying and tracking new classes of threats. Due to the increasing flexibility and reprogramability of modern electronics, new RADAR and communications systems can modify pulse and frequency emission characteristics on very short time scales in such a manner that existing EW systems cannot correctly detect and classify threats based on these new electronics. The photonically sampled imaging receiver technology being investigated as part of this effort could potentially address this problem by providing a new class of receiver that sorts incoming radiation by Angle of Arrival (AoA) prior to signal analysis. Since AoA for these threats cannot readily be changed, an EW system that first sifts received signals on this basis could be potentially advantageous. To this end, the PI participated in a study of a potential EW/RWR system in comparison with an existing representative electronic system based on current installed implementations. Specifically, a comparison of the optically sampled imaging receiver to the Rockwell-Collins CS-3120 system was performed. The Rockwell Collins CS-3120, was chosen as a representative RWR system, as it is representative of many of the larger class of RWR receiver and specifications for the system were available to the public domain.

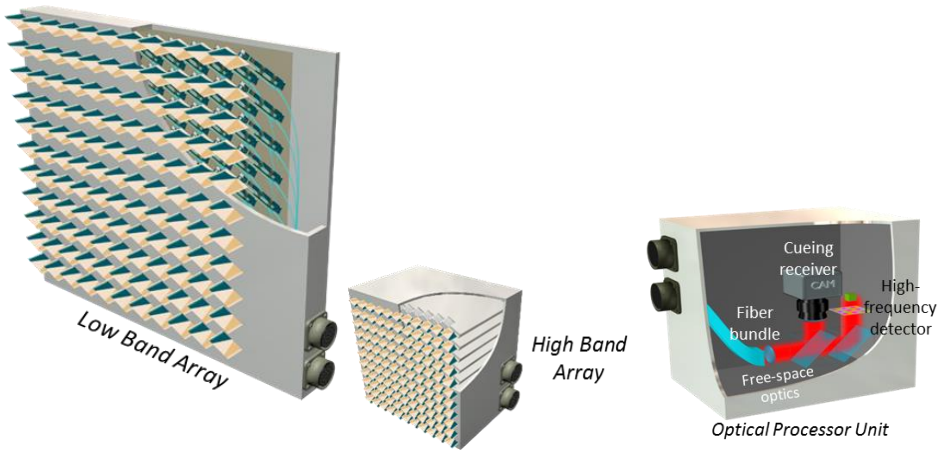

Figure 18. Representative drawings of low-band array (7-20 GHz), high band array (20-60 GHz), and there associated optical processor.

Based on the capabilities of this receiver, the PI helped to develop a notional RWR receiver based on the photonically sampled coupled antenna array that is the focus of this effort. For this analysis, we considered primarily technologies that could be realized within the next three-five years. The results of this notional receiver design are shown in Figure 18.

From this notional receiver design, performance parameters were predicted based on initial models of system performance. These models assumed that sufficient LNA gain was used on the antenna to set the noise floor of the imaging receiver, which necessitated physical area behind the antenna to allow for this integration. Additionally, use of optical modulators to encode the signals based on lithium niobate require a linear length on the order of 1". Based on an area for these LNA's and modulator of about one square inch, an architecture was chosen which was densely packed at the highest frequency of operation for each of two banded arrays. To achieve this packing density the high band array (20-60 GHz) required out of plane integration, which yielded an approximate depth of 3", while the low band (7-20 GHz) array uses in plane integration with slotted dipole antenna to achieve an approximate depth of one inch. Overall the anticipated performance of these array was compared with the CS-3120 and the results are shown in Figure 19.

Key aspects of this comparison are that the imaging array provides significant benefit in many areas over the existing RWR system. Key among them are:

- The ability to discriminate AoA in two dimensions.
- Increased sensitivity and/or increased AoA resolution
- Larger instantaneous bandwidth
- Ability to resolve multiple threats within the same frequency band
- Lower size, weight, and power consumption

While these studies yielded several key advantages of the proposed approach, this technology is still deficient in a couple of key areas. First, the free space optical filters used to reject the optical carrier limit the low end operational frequency of this technique to an estimated 7-10 GHz, which is insufficient for many EW applications. Second, the packing density of the required support circuitry is insufficient to create the desired conformal form factors that could be potentially be realized by this optically sampled approach and even the proposed arrays required significant reductions in the optical upconversion and amplifiers front ends. To this end, the PI participated in efforts to both improve the integration density of these arrays and reduce the low end operating frequency. Efforts to increase integration density focused primarily on liquid crystal polymer as substrate for heterogeneous integration of RF and optical components as described in the following section. A number of potential solutions were identified to address reaching low frequencies using the optical imaging receiver approach including, but not limited to, single-sideband suppressed-carrier modulators, RF upconversion prior to modulation, and high resolution fiber based optical filters. Section 6 discusses recent efforts to create a wideband imaging receiver covering several octaves using suppressed carrier optical modulators to extend the frequency response of this imaging receiver technique down to 4 GHz.

Systems	CS-3120* 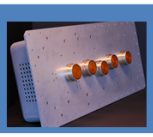	Imaging receiver 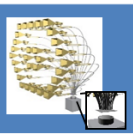
Frequency range (GHz)	2-18	7-60
Angular resolution (degree)	N/A	6 @7GHz
Direction finding accuracy (degree)	< 1 Azimuthal only (1-D)	< 0.5 Azimuth and Elevation (2-D)**
Azimuthal FOV (degree)	120 (± 60)	120 (± 60)
Elevation FOV (degree)	20 (± 10)	120 (± 60)
System sensitivity	-65dBm (500MHz BW)	-75 dBm (500MHz BW) **
IF output channels	4	N/A
RF output channels	1	N/A
Polarization	Circular polarization	Linear or Circular polarization
Size	27'' x 12'' x 6'' Front End Only	13" x 10" x 3"
Weight	30 lbs Front End Only	25 lbs Including Processor
Power	70 W Front End Only (700W Total)	~200W Including Processor
IBW (GHz)	0.5	Up to 60
Instantaneous multi-beams	1	100 ~ 1000

*Comparable systems include ITT SE129, SE131, and Excelis SE135 series.
**Sensitivity and DF accuracy can be traded to limits of -85 dBm sensitivity or 0.25° DF accuracy.

Figure 19. Comparison of current standard RWR and optically based imaging receiver concept.

5 INVESTIGATED TECHNIQUES FOR INTEGRATING ANTENNAS AND OPTICAL UPCONVERSION DEVICES

To achieve the integration density required to realize the desired densely packed EW receivers described in the previous section, new techniques for component integration had to be developed. As shown in Figure 20, the current RF front-end modules used in the Pathfinder array utilized COTS piece parts which, despite being optimized for minimal spacing between antenna still set the minimum pitch of the antennas at ~4".

Figure 20. RF Front-End Module in current Pathfinder imaging receiver demonstration system with a length of ~14" and a 3" diameter with protrusions that set the minimum pitch of the array to ~4". From left two right, components of chain include horn antenna, waveguide based low noise amplifier, and COTS optical modulator embedded in plastic holding cylinder.

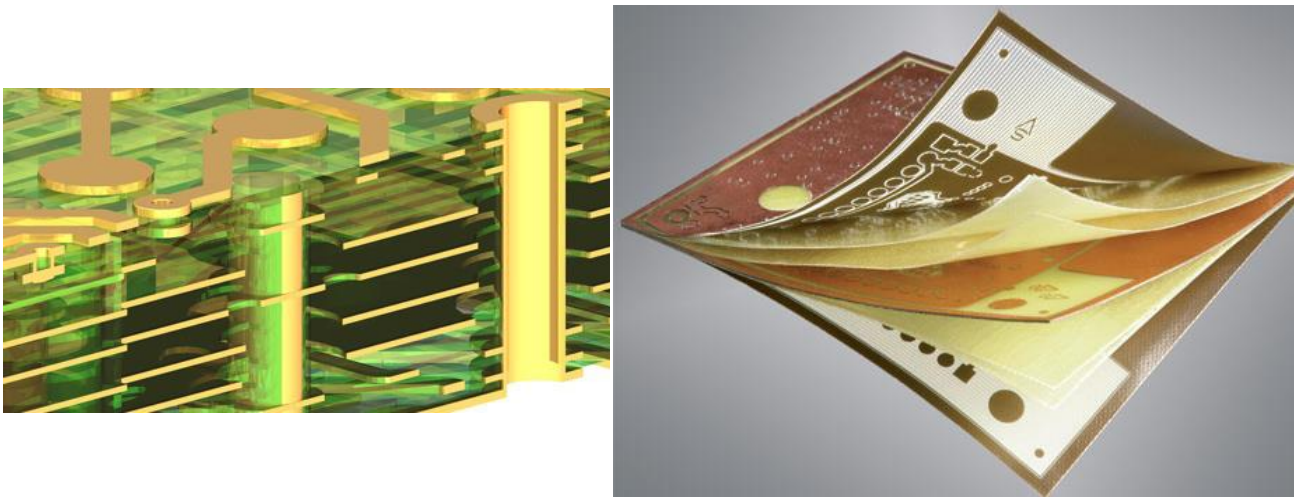

Figure 21. Conductive layers all interconnected to each other through coupling structures (left) and the LCP material (right)

To enable the realization of the types of dense designs of interest to these receivers, the PI participated in development work to design an integrated RF front-end module that would contain all of the essential components: antenna, LNAs, and modulator in a cost effective manner. This effort led to the design and fabrication of multilayer liquid crystal polymer (LCP) circuits. Multilayer LCP consists of bonded conductive layers that are interconnected by means of plated through-holes or coupling structures such as in Figure 21 (left). The new module architecture introduced many advantages over the original modules. Advantages include a low profile design, light weight, low loss, low power consumption, and extreme flexibility. Figure 21 (right) illustrates the paper-like material suitable for RF frequencies up to 110 GHz.

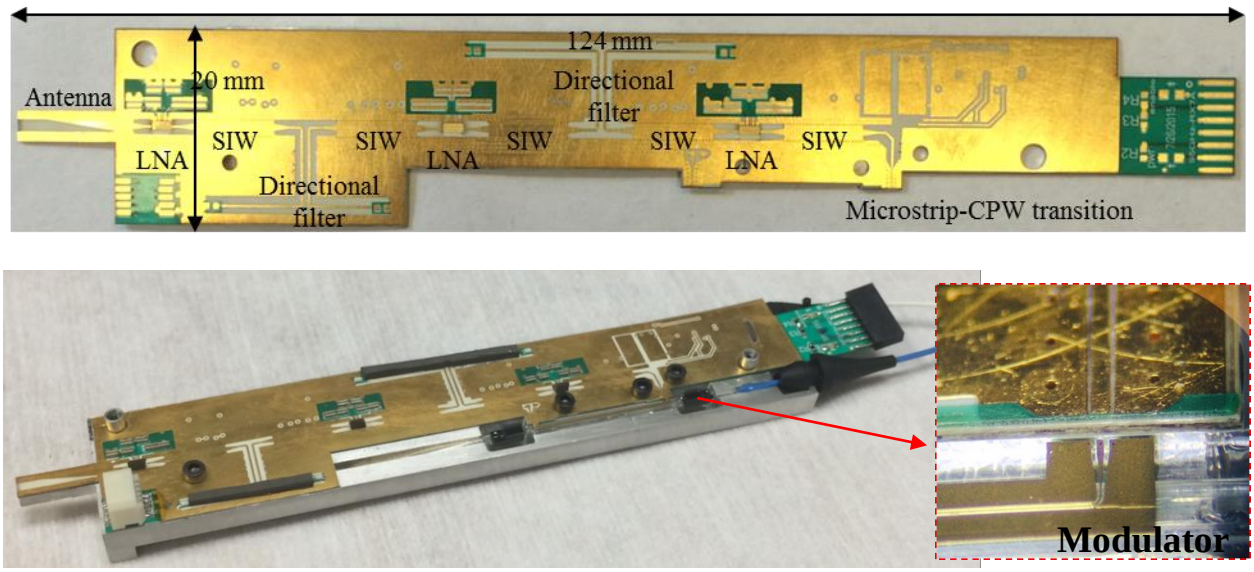

Figure 22. Detailed LCP module with all of the RF components labeled (top) and a package LCP RF Front-End module with an integrated electro-optic modulator (bottom)

LCP allows the integration of efficient waveguides, filters, power splitter, and antennas to be fabricated in this material using standard printed circuit board manufacturing techniques. The active components such as the low noise amplifiers (LNAs), LO generators, and mixers as well as the biasing electronics can also be incorporated in the same substrate. A key aspect of this approach to component integration is that, unlike traditional microwave and millimeter-wave packaging techniques, most of the critical dimensions of the electronic circuits, transitions, and transmission lines are lithographically defined in a single substrate using printed wiring board techniques that are subject to very favorable economies of scale.

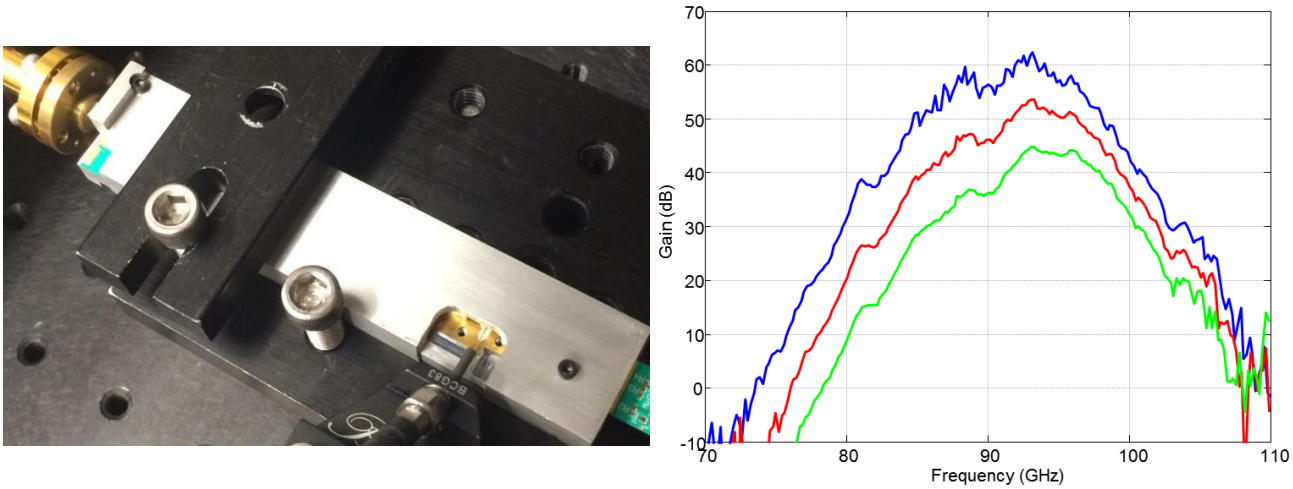

Figure 23. Packaged LCP module with a ground-signal-ground probe on the output of the modulator to test the optical upconversion process (left) and the gain curves of three packaged and tested modules at various bias conditions (right).

Over the course of this effort, we participated in several design efforts that contributed to the realization of a fully integrated frontend module in a single LCP based package. A description of the components on the LCP module as well as the overall packaged module is shown in Figure 22 (top). The module in Figure 22 (bottom) comprises three LCP layers and four circuit layers. The RF components are designed in the top two layers, including LNAs, directional filters, microstrip-CPW transition, substrate integrated waveguides (SIWs), and microstrip to SIW transitions. These modules were designed to operate in W-band centered on the 94 GHz window in pursuit of a related pmmW imaging program. The same techniques could be applied to the realization of the broadband receiver modules necessary to realize the array laid out conceptually during the trade study effort, however, realization of the full design of these modules was not achievable within the resource constraints of this effort.

The modules shown in Figure 22 consisted of three LNA gain stages with surface integrated waveguide transitions and directional filters between each stage to provide the narrowband high gain response necessary for pmmW operation. Testing of these modules prior to integration of the optical modulator as shown in Figure 23 has shown module RF gains in excess of 60 dB without oscillation.

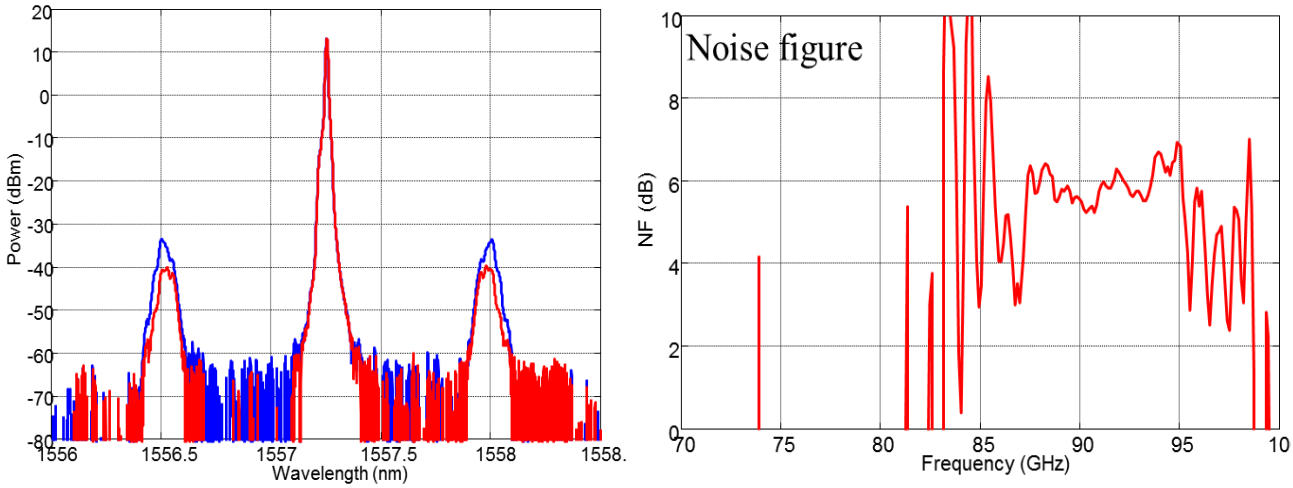

Figure 24. Optical Spectrum of the upconverted RF onto sidebands without (red) and with (blue) a noise source on (left) and the corresponding noise figure of the modules designed to operate at 94 GHz (right)

After testing of RF gain, the modules have been integrated with a high speed optical modulator designed and fabricated at the University of Delaware in conjunction with colleagues at Phase Sensitive Innovations, Inc. Figure 24 shows optical spectrum of the fiber output of a completed module. To measure noise figure, we constructed a Y-factor optical sideband setup to receive optical sideband power with and without a calibrated noise diode on at the RF input of the module. Noise figure results can then be extracted from difference in sideband strength. Figure 24 (left) shows the optical spectrum with the noise source off (red) and on (blue) and the resulting noise figure of the module (Figure 24 (right)). To date, roughly twenty five of these modules have been fabricated and have demonstrated consistency in gain and noise performance.

6 LOW BAND RECEIVER REALIZATION

One of the known major limitations of the imaging receiver is that it imposes the necessity of filtering the optical carrier prior to image formation. In all prior incarnations of the imaging receiver, the low end of the microwave frequency range that could be accessed was limited by the optical filters that filtered the carrier from the sideband. Even using cascades of state-of-the-art dense wavelengths division multiplexing filters, providing rejection of the optical carrier frequency without significantly attenuating the imaged sidebands required a separation of the optical sidebands of at least 10 GHz for reasonable rejection ratios. To this end, we began to investigate other techniques for rejecting the optical carrier. The most successful approach came from using high extinction ratio Mach-Zehnder type intensity (MZI) modulators to replace the phase modulators previously being used for upconversion, and biasing these modulators at the point of minimum transmission. Using these techniques in conjunction with modern commercially available MZI's enabled 30 dB of carrier rejection directly out of the modulator output. Based on this technique, we contributed to building a proof-of-concept 1x4, broadband imaging array as shown in Figure 25.

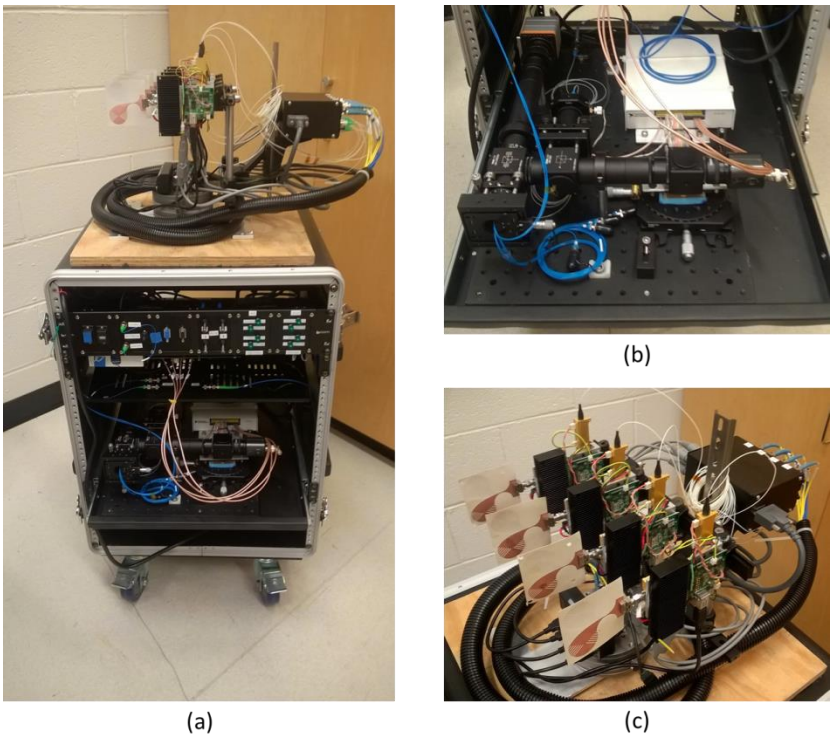

Figure 25 1x4 Imaging Receiver as presently constructed. (a) Overview image showing the antenna head assembly atop the wheeled rack containing the power and processing subsystems. (b) View of the free-space optical system. (c) Close-up view of the antenna & modulator array mounted on a rotating stage, with each module comprising an antenna, LNA, modulator and bias controller.

A complete system schematic diagram is shown in Fig. 26. This system utilizes four 40-GHz commercial MZI amplitude modulators, fed by custom fabricated wideband antipodal Vivaldi antennas, with wideband, high-gain, low-noise amplifiers (LNAs). Each of these components was selected for its ability to cover the bandwidth from 4- 40 GHz. The laser source is a 100-mW commercial DFB laser, optionally boosted by an erbium doped fiber amplifier (EDFA). Carrier suppression for low-frequency imaging is performed by a combination of null-biasing the modulators, along with cascaded DWDM filters.

Control of the system is achieved through a combination of manual instrument panel switches and a PC-based user interface built with National Instruments LabVIEW software running on a PC. Separate PC based software is used to configure the modulator bias controllers, which are required to monitor the bias condition of the modulators and continuously compensate for bias drift to maintain carrier nulling. The control system includes a closed-loop phase-stabilization subsystem to actively compensate for phase variations induced by the environmental perturbations to the loose optical fibers. This phase-locking system was adapted from the one utilized in the Pathfinder imager.

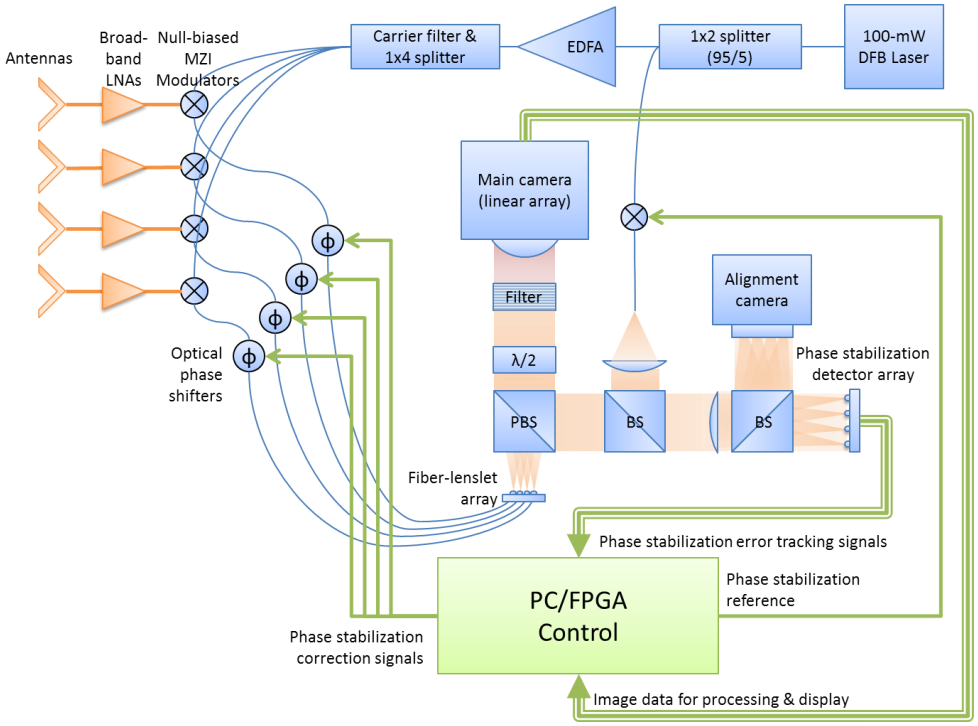

Figure 26 Diagram of the 1x4 low band imaging receiver system.

Using this setup, we have been able to demonstrate detection and location of sources from 4- 40 GHz imaged onto the linear camera array. As shown in Figure 27, line spread functions formed from imaging an RF source were taken over a range of angles and emission frequencies. These images were taken without recalibration of the optical phases within the array, and shown clear detection and location of the source within the limits of the 1x4 array layout. As the frequency is increased the relative positions of detection on the camera shift away from the center of the image. This achromaticity of the image reformation was anticipated and is derived from the relative scaling of the antenna spacing to the optical fiber array spacing. As the source progresses off the normal axis of the imager, a relative time delay is introduced between elements of the array that results in a frequency dependent phasing of the collected RF energy. From an imaging perspective, this results in a linear scaling of the image as a function of the RF frequency. This effect is readily apparent in the data in Figure 27, where the number of pixels corresponding to an angular shift of the incoming RF source is increased by roughly a factor of four as the frequency is increased by two octaves from 7.4 GHz to 36 GHz. Also for sources on axis, note that reconstructed image position does not change as a function of frequency. At first, such achromaticity seems to complicate source location of angle of arrival calculation for a given source. However, since this scaling is deterministic and can be adjusted by tuning the relative fiber lengths of the optical feed to the processor, it is possible to use this scaling to simultaneously unique locate both angle of arrival and frequency of emission incident on the array. Developments made under this effort have fed into follow-on programs that are attempting to

formalize these techniques, which will use multiple fiber paths to provide both AoA and frequency from a single imaging receiver aperture.

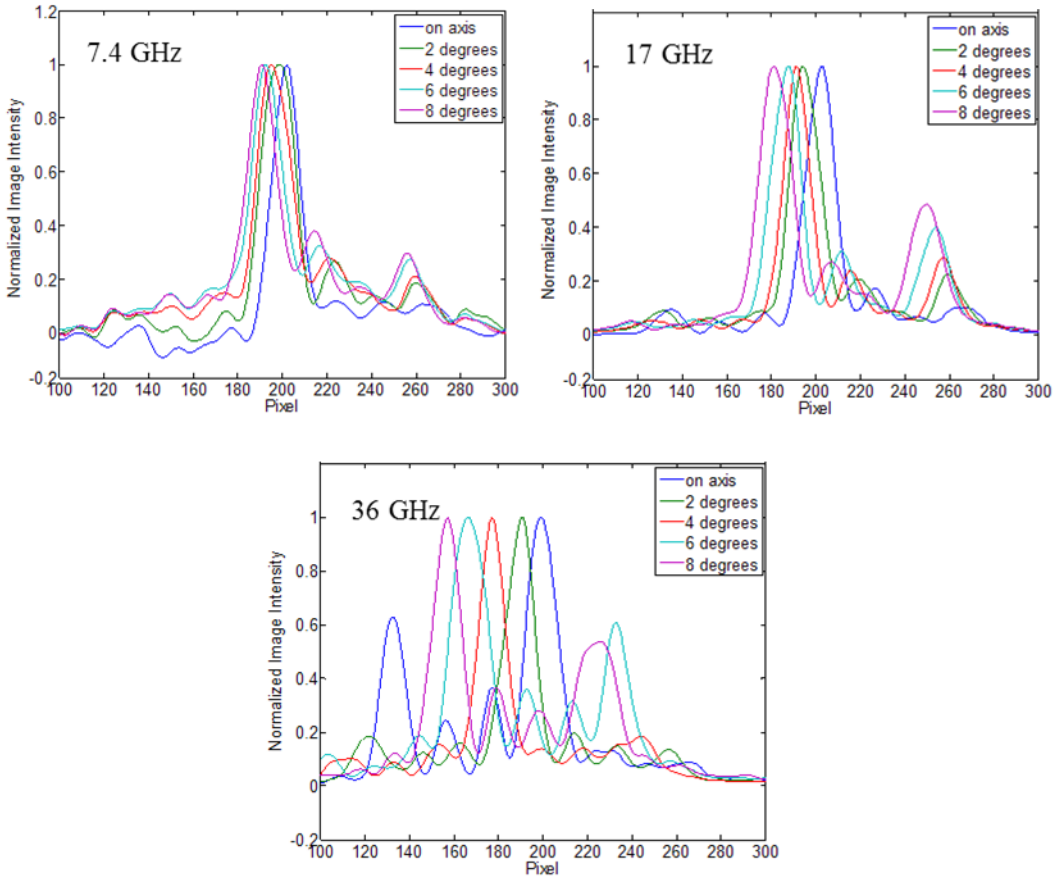

Figure 27 Chromatic dispersion in the wideband imaging receiver. Plots are normalized to emphasize the lateral shift of the peaks as frequency increases.

7 SUMMARY OF ACCOMPLISHMENTS AND RESULTS

Over the course of this effort, to our knowledge, we have realized the first ever imaging receiver capable of simultaneously forming all available beams from a phased array based on optical sampling and image reconstruction. This "imaging receiver" technology has been shown to provide sensitivities sufficient to image the thermal noise floor and will provide new capabilities as a broadband electronic warfare cueing receiver. Additionally, we have demonstrated the capability of this imaging receiver technology to spatially isolate and recover both baseband and optically downconverted RF signals. This optical downconversion has been enabled by introducing an injection-locked paired source, which was built and tested under this effort. This paired source allowed the imaging receiver to achieve ultra-wideband frequency identification at an IF suitable to off the shelf test equipment and high-powered low speed photodiodes while having the capability of adjusting the downconversion frequency over several octaves of bandwidth. We have demonstrated this receiver approach has the capability of locating, recovering, and analyzing electronic emissions while suppressing unwanted co-channel interference. More specifically, we have demonstrated the capability to recover complexly encoded communications waveforms in the presence of emitters in the same band, utilizing the spatial filtering capabilities of the imaging receiver.

Based on these demonstrations, we have explored concepts for novel electronic warfare receivers and compared them against publicly available specifications for currently available electronic support systems and RADAR warning receivers. Using these trade studies, we have developed a notional receiver concept and identified key technology areas that must be advanced to realize these receivers. Among these key technology areas were integrated RF/optical frontends and techniques for reducing the low end frequency capabilities of the imaging receiver technique. On both of these fronts hardware was developed and proven that significantly advanced the capabilities to realize such arrays.

The successes generated under this effort have already led to several follow-on efforts. Most notably a five year development program with AFRL-RX (Rob Nelson) is exploring the use of these technologies for Air Force application multifunctional conformal apertures. This program, which is already underway, will produce hardware demonstration systems of both these imaging receiver and a related optically driven broadband phased array transmitter technology to be tested at Wright Patterson AFB starting in FY16.

7.1 Resulting Publications and Patents

1) G. J. Schneider, J. A. Murakowski, C. A. Schuetz, S. Shi, and D. W. Prather, "Radiofrequency signal-generation system with over seven octaves of continuous tuning," *Nature Photonics*, vol. 7, no. 2, pp. 118–122, 2013.
2) J. N. Mait, R. D. Martin, C. A. Schuetz, and D. W. Prather, "Millimeter wave imaging with engineered point spread functions," *Optical Engineering*, vol. 51, no. 9, 2012.
3) S. Shi, J. Bai, G. J. Schneider, Y. Zhang, R. Nelson, J. Wilson, C. Schuetz, D. W. Grund Jr., and D. W. Prather, "Conformal wideband optically addressed transmitting phased array with photonic receiver," *Journal of Lightwave Technology*, vol. 32, no. 20, pp. 3468–3477, 2014.
4) S. Shi, C. Schuetz, R. Martin, T. Dillon, P. Yao, J. Murakowski, G. Schneider, and D. W. Prather, "System modeling of passive millimeter wave imager based on optical up-conversion," in *Physics and Simulation of Optoelectronic Devices XX, January 23, 2012 - January 26, 2012*, 2012, vol. 8255, p. The Society of Photo–Optical Instrumentation Engineers (SPIE).
5) B. M. Overmiller, C. A. Schuetz, G. Schneider, J. Murakowski, and D. W. Prather, "Ultrabroadband phased-array radio frequency (RF) receivers based on optical techniques," in *Terahertz, RF, Millimeter, and Submillimeter-Wave Technology and Applications VII, February 4, 2014 - February 6, 2014*, 2014, vol. 8985, p. Hubner GmbH and Co. KG; The Society of Photo–Optical Instrumentation Engineers (SPIE).
6) J. N. Mait, R. D. Martin, C. A. Schuetz, S. Shi, D. W. Prather, P. F. Curt, and J. Bonnett, "Minimum bias design for a distributed aperture millimeter wave imager," in *2013 1st IEEE Global Conference on Signal and Information Processing, GlobalSIP 2013, December 3, 2013 - December 5, 2013*, 2013, pp. 711–714.
7) G. J. Schneider, J. Murakowski, C. A. Schuetz, S. Shi, and D. W. Prather, "Widely tunable narrow-line RF source based on modulation sideband injection-locked lasers," in *2013 IEEE International Topical Meeting on Microwave Photonics, MWP 2013, October 28, 2013 - October 31, 2013*, 2013, pp. 261–263.
8) S. Shi, J. Bai, G. Schneider, Y. Zhang, R. Nelson, J. Wilson, C. Schuetz, and D. Prather, "Conformal ultra-wideband optically addressed transmitting phased array and photonic receiver systems," in *2013 IEEE International Topical Meeting on Microwave Photonics, MWP 2013, October 28, 2013 - October 31, 2013*, 2013, pp. 221–224.
9) J. Murakowski, G. J. Schneider, C. A. Schuetz, S. Shi, and D. W. Prather, "Linearized broadband optical detector: Study and implementation of optical phase-locked loop," in *Photonics West 2014 Conference on Broadband Access Communication Technologies VIII, February 4, 2014 - February 6, 2014*, 2014, vol. 9007, p. The Society of Photo–Optical Instrumentation Engineers (SPIE).
10) D. W. Prather, J. Murakowski, G. J. Schneider, C. Schuetz, and S. Shi, "Emerging millimeter wave photonic devices and integration platforms for avionic applications," in *2014 IEEE Avionics, Fiber-Optics and Photonics Technology Conference, AVFOP 2014, November 11, 2014 - November 13, 2014*, 2014, pp. 25–26.

Patent Disclosures

1) Patent Disclosure Submitted through UD, 6/2014, "Spatially discriminating phased-array radio receiver with enhanced dynamic range and jamming immunity." Patent Pending.

1.

1. Report Type

Final Report

Primary Contact E-mail

Contact email if there is a problem with the report.

cschuetz@udel.edu

Primary Contact Phone Number

Contact phone number if there is a problem with the report

610-662-1075

Organization / Institution name

University of Delaware

Grant/Contract Title

The full title of the funded effort.

Ultrabroadband Phased-Array Receivers Based on Optical Techniques

Grant/Contract Number

AFOSR assigned control number. It must begin with "FA9550" or "F49620" or "FA2386".

FA9550-12-1-0380

Principal Investigator Name

The full name of the principal investigator on the grant or contract.

Dr. Christopher Schuetz

Program Manager

The AFOSR Program Manager currently assigned to the award

Dr. Gernot Pomrenke

Reporting Period Start Date

07/15/2012

Reporting Period End Date

07/14/2015

Abstract

Military operations require the ability to locate and identify electronic emissions in the battlefield environment. However, developments in RADAR and communications technology are making it harder to effectively identify these broadband and increasingly dynamic emissions. To this end, under this effort a broadband imaging receiver for the location and identification of microwave and millimeter-wave emitters has been developed. This approach utilizes photonic techniques to realize an imaging receiver that enables us to capture and convert signals across an array using photonic modulators, routing these signals to a central location using fiber optics, and spatially and spectrally processing the incoming signals using simple free space optics. Over the course of this effort, the capability of using such an optically enabled imaging receiver array to simultaneously detect, locate, and downconvert multiple high-gain beams in a non-blocking fashion using an optically enabled imaging receiver array has been demonstrated for the first time. This technology was demonstrated first by adapting an existing 35 GHz passive millimeter wave imager that predated this effort, and subsequently by building a four element broadband array, which is capable of detection over the range of 4-50 GHz.

Distribution Statement

This is block 12 on the SF298 form.

Distribution A - Approved for Public Release

Explanation for Distribution Statement

If this is not approved for public release, please provide a short explanation. E.g., contains proprietary information.

SF298 Form

Please attach your SF298 form. A blank SF298 can be found here. Please do not password protect or secure the PDF The maximum file size for an SF298 is 50MB.

SF298_FA9550-12-1-0380.pdf

Upload the Report Document. File must be a PDF. Please do not password protect or secure the PDF . The maximum file size for the Report Document is 50MB.

FA9550-12-1-0380_YIP Final Report.pdf

Upload a Report Document, if any. The maximum file size for the Report Document is 50MB.

Archival Publications (published) during reporting period:

1) G. J. Schneider, J. A. Murakowski, C. A. Schuetz, S. Shi, and D. W. Prather, "Radiofrequency signal-generation system with over seven octaves of continuous tuning," Nature Photonics, vol. 7, no. 2, pp. 118–122, 2013.
2) J. N. Mait, R. D. Martin, C. A. Schuetz, and D. W. Prather, "Millimeter wave imaging with engineered point spread functions," Optical Engineering, vol. 51, no. 9, 2012.
3) S. Shi, J. Bai, G. J. Schneider, Y. Zhang, R. Nelson, J. Wilson, C. Schuetz, D. W. Grund Jr., and D. W. Prather, "Conformal wideband optically addressed transmitting phased array with photonic receiver," Journal of Lightwave Technology, vol. 32, no. 20, pp. 3468–3477, 2014.
4) B. M. Overmiller, C. A. Schuetz, G. Schneider, J. Murakowski, and D. W. Prather, "Ultrabroadband phased-array radio frequency (RF) receivers based on optical techniques," in Terahertz, RF, Millimeter, and Submillimeter-Wave Technology and Applications VII, February 4, 2014 - February 6, 2014, 2014, vol. 8985, p. Hubner GmbH and Co. KG; The Society of Photo–Optical Instrumentation Engineers (SPIE).
5) J. N. Mait, R. D. Martin, C. A. Schuetz, S. Shi, D. W. Prather, P. F. Curt, and J. Bonnett, "Minimum bias design for a distributed aperture millimeter wave imager," in 2013 1st IEEE Global Conference on Signal and Information Processing, GlobalSIP 2013, December 3, 2013 - December 5, 2013, 2013, pp. 711–714.
6) G. J. Schneider, J. Murakowski, C. A. Schuetz, S. Shi, and D. W. Prather, "Widely tunable narrow-line RF source based on modulation sideband injection-locked lasers," in 2013 IEEE International Topical Meeting on Microwave Photonics, MWP 2013, October 28, 2013 - October 31, 2013, 2013, pp. 261–263.
7) S. Shi, J. Bai, G. Schneider, Y. Zhang, R. Nelson, J. Wilson, C. Schuetz, and D. Prather, "Conformal ultra-wideband optically addressed transmitting phased array and photonic receiver systems," in 2013 IEEE International Topical Meeting on Microwave Photonics, MWP 2013, October 28, 2013 - October 31, 2013, 2013, pp. 221–224.
8) J. Murakowski, G. J. Schneider, C. A. Schuetz, S. Shi, and D. W. Prather, "Linearized broadband optical detector: Study and implementation of optical phase-locked loop," in Photonics West 2014 Conference on Broadband Access Communication Technologies VIII, February 4, 2014 - February 6, 2014, 2014, vol. 9007, p. The Society of Photo–Optical Instrumentation Engineers (SPIE).
9) D. W. Prather, J. Murakowski, G. J. Schneider, C. Schuetz, and S. Shi, "Emerging millimeter wave photonic devices and integration platforms for avionic applications," in 2014 IEEE Avionics, Fiber-Optics and Photonics Technology Conference, AVFOP 2014, November 11, 2014 - November 13, 2014, 2014, pp. 25–26.
Patent Disclosures
1) Patent Disclosure Submitted through UD, 6/2014, "Spatially discriminating phased-array radio receiver with enhanced dynamic range and jamming immunity." Patent Pending.

Changes in research objectives (if any):

None

Change in AFOSR Program Manager, if any:

None

Extensions granted or milestones slipped, if any:

None

AFOSR LRIR Number

LRIR Title

Reporting Period

Laboratory Task Manager

Program Officer

Research Objectives

Technical Summary

Funding Summary by Cost Category (by FY, $K)

	Starting FY	FY+1	FY+2
Salary			
Equipment/Facilities			
Supplies			
Total			

Report Document

Report Document - Text Analysis

Report Document - Text Analysis

Appendix Documents

2. Thank You

E-mail user

Mar 01, 2016 09:54:39 Success: Email Sent to: cschuetz@udel.edu